

# We are IntechOpen, the world's leading publisher of Open Access books Built by scientists, for scientists

6,900

Open access books available

186,000

International authors and editors

200M

Downloads

Our authors are among the

154

Countries delivered to

TOP 1%

most cited scientists

12.2%

Contributors from top 500 universities



WEB OF SCIENCE™

Selection of our books indexed in the Book Citation Index  
in Web of Science™ Core Collection (BKCI)

Interested in publishing with us?  
Contact [book.department@intechopen.com](mailto:book.department@intechopen.com)

Numbers displayed above are based on latest data collected.  
For more information visit [www.intechopen.com](http://www.intechopen.com)



---

# Bandwidth Enhancement Techniques

---

Seyed Ali Razavi Parizi

Additional information is available at the end of the chapter

<http://dx.doi.org/10.5772/intechopen.70173>

---

## Abstract

In this chapter, a variety of procedures proposed in the literature to increase the impedance bandwidth of microstrip patch antennas are presented and discussed. Intrinsic techniques, proximity coupled and aperture-coupled patches, applying horizontally coupled patches to driven patch on a single layer and stacked patches are discussed. Beside the linear polarised solutions, some techniques for designing wideband circular polarised patch antennas are also presented. Furthermore, some other techniques proposed in the literature including log-periodic array of patches, E-shaped patch, L-shaped feeding, microstrip monopole slotted antenna, defected ground/patch technique and the latest works during the recent years are introduced and investigated. It is tried to make a comparison between different methods giving a typical bandwidth that can be obtained using each method, beside discussing about the benefits or limitations that each method has.

**Keywords:** bandwidth enhancement, microstrip patch antenna, aperture coupled, stacked patches, non-contact feeding, parasitically coupled, sequential rotated array

---

## 1. Introduction

Microstrip patch antennas, in their conventional form, are narrow-band structures. Their impedance bandwidth is typically 1–2%. This can be attributed to two factors: the resonant style of antenna (which makes the antenna radiate efficiently only over a narrow band of frequencies) and the thin thickness of antenna, typically less than  $0.05\lambda_0$ .

This feature of conventional microstrip patch antennas makes them unsuitable in many applications where quite wide bandwidth is required. So, many researches have been done during the past few decades to overcome this limitation and several procedures have been proposed.

In this chapter, we will describe the most useful procedures proposed in the literature to increase the impedance bandwidth of microstrip patch antennas. In Section 2, the intrinsic

---

techniques which can be used to increase the bandwidth of a single layer direct fed microstrip patch antenna are described. Section 3 investigates different feeding techniques used for bandwidth enhancement of microstrip patch antennas. In the proposed techniques, the antenna structure is multilayered and the patch is fed by a non-contact feed network. In Section 4, bandwidth enhancement by use of horizontally parasitic elements at the antenna aperture will be described. Sections 5 and 6 explore the stacked patches, a multilayered solution using vertically parasitic elements that can result in very wide bandwidths. In Sections 2–6, the focus is on linear polarised antennas. So, the solutions for wideband circular polarised patch antennas are introduced and discussed in Section 7. Finally, in Section 8, other techniques proposed in the literature including log-periodic array of patches, E-shaped patch, L-shaped feeding and microstrip monopole slotted antenna are introduced and investigated.

In this chapter, we tried to discuss about the principles of operation of presented antennas to give the reader insight into how these antennas work. Some examples are also given. The advantages and limitations of each method will be described and a comparison between them will be provided by giving the typical order of bandwidth that can be achieved using each method. By this way, in this chapter, it is tried to provide a designer's prospective of different techniques used for bandwidth enhancement of microstrip patch antennas.

## 2. Intrinsic techniques

Two intrinsic procedures can be applied to improve the bandwidth of a single layer direct fed microstrip patch antenna. One is increasing the substrate thickness and the other is decreasing the dielectric constant of antenna substrate (relative permittivity of near to one). This can also be observed in **Figure 1**, in which the bandwidth trends of a direct fed single layer microstrip patch relative to substrate permittivity and thickness are shown.

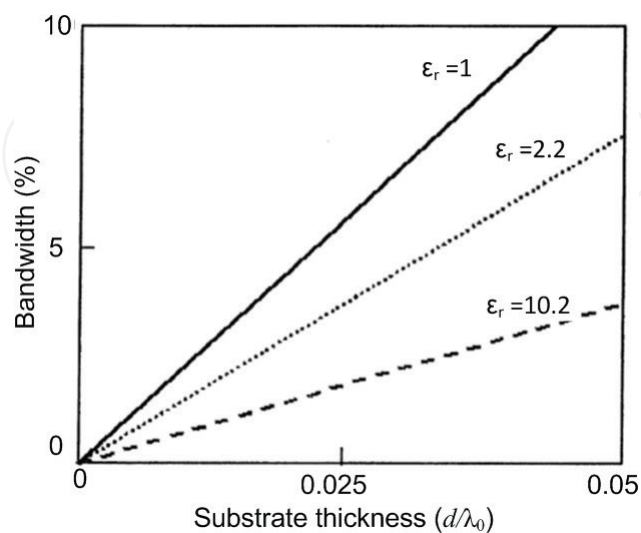


**Figure 1.** Bandwidth trends of a direct fed single-layer microstrip patch relative to substrate permittivity and thickness [1].

In fact, by increasing the thickness of the radiating patch substrate, the aperture size through which the fields are radiating to the space can be enhanced leading to easier impedance matching of antenna aperture which results in antenna bandwidth enhancement. On the other hand, by decreasing the substrate permittivity (making it closer to the permittivity of outer space), the reflection coefficient at the antenna aperture is reduced making it easier to impedance match which provides wider bandwidth for the antenna.

It should be noted that as the thickness of the substrate is increased and the dielectric constant is reduced, the patch size becomes smaller which provides lower gain. In addition, the radiated power by feed network increases leading to more spurious radiation and higher cross-polarisation level. Furthermore, the surface waves are more excited reducing the antenna radiation efficiency.

Taking the abovementioned limiting factors into consideration, besides the fact that there are limited values for thicknesses and dielectric constants provided by standard commercial substrates, the bandwidth enhancement by the mentioned intrinsic techniques cannot exceed 10% [2] which is still not adequate for many applications like L-band radar which needs 19% bandwidth (1.4–1.7 GHz) or C-band satellite TV that requires 12.5% bandwidth (3.7–4.2 GHz). So, other techniques as mentioned at the following must be applied to enhance the bandwidth more.

### 3. Feeding techniques

In all proposed feeding techniques presented in this section, the antenna structure is multi-layered and the radiating patch is fed by a non-contact feed network. In fact by introducing a coupling mechanism between the feed network and patch, a resonance is created at the vicinity of patch resonance which can result in antenna bandwidth enhancement if the feed network and patch are well coupled.

#### 3.1. Proximity coupled feed

In **Figure 2**, topology of proximity coupled feeding is depicted. In this feeding mechanism, the radiating patch on the upper layer (radiating layer) is excited by an open-ended microstrip feed line printed on the lower layer (feed layer). It can be seen that there is no direct contact

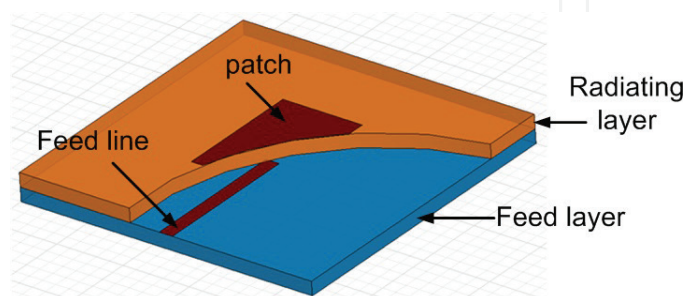


**Figure 2.** Topology of proximity coupled feed.

between feed line and radiating patch. So, the fields are coupled to the patch via the open end of stub. By tuning the location of open end of feed line relative to the patch, a proper coupling between them can be obtained leading to expansion of antenna bandwidth. By this way, the bandwidth at the order of 8% can be achieved.

In order to increase the bandwidth more, we can increase the thickness of radiating layer. However, this makes the coupling of power from the feed network to the patch more difficult. To solve this problem, thicker substrate for the feed layer can be used. In this case, more power is coupled to the patch via open circuit stub, but at the same time, the spurious radiation caused by feed network becomes more severe which can degrade the antenna efficiency. Another solution for this issue is applying a simple matching structure, for example, a quarter-wave transformer, to the feed line. By this way, i.e. using thicker laminate for the radiating layer besides applying matching circuit to the feed network, the bandwidth can be doubled [1]. In **Figure 3**, one example about this issue is presented [1]. In this example by doubling the thickness of radiating layer and using a simple impedance transformer at the feed line, the bandwidth could be enhanced from 8 to 14%.

### 3.2. Aperture-coupled feed

In **Figure 4**, the topology of aperture-coupled feeding is depicted. In this feeding mechanism, the radiating patch on the upper layer (radiating layer) is excited by a microstrip feed line printed on the lower layer (feed layer) via an aperture (slot) etched at the ground plane of radiating layer.

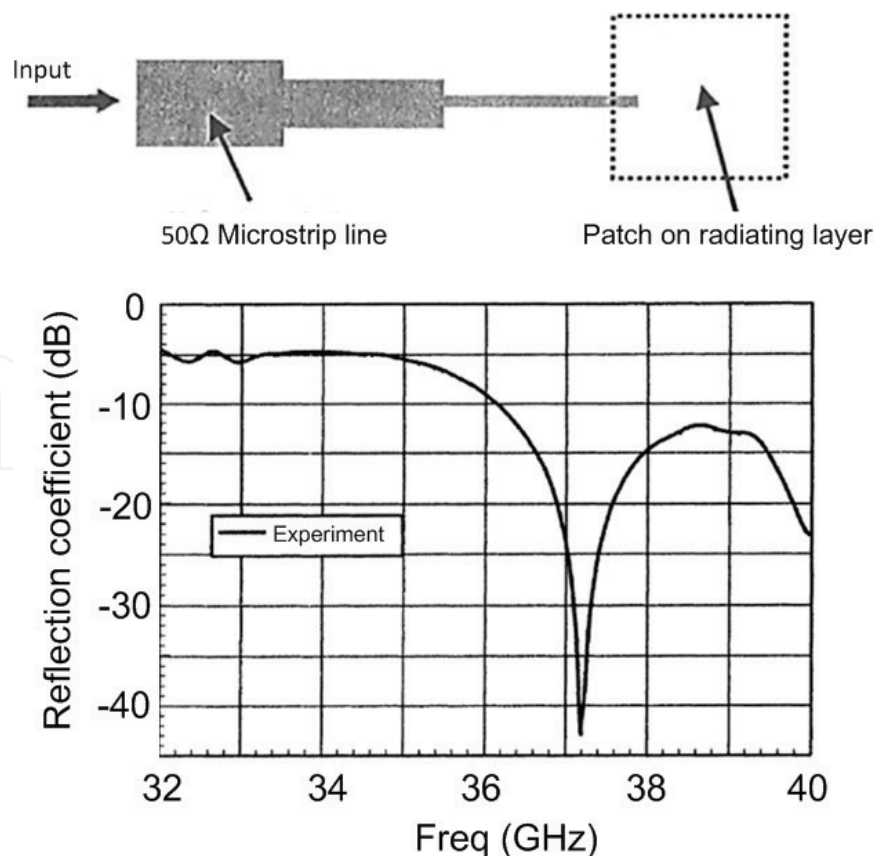


**Figure 3.** S11 of a proximity coupled microstrip patch antenna presented in Ref. [1].

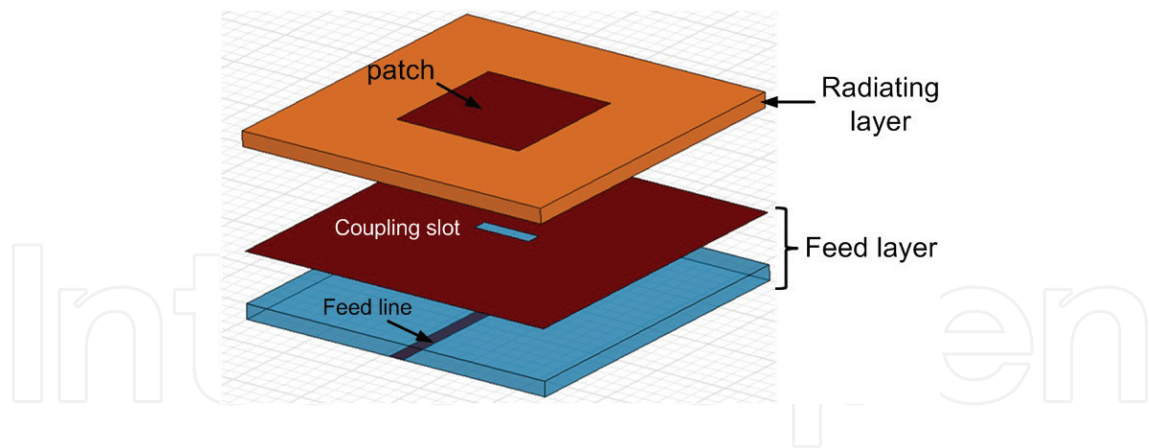


**Figure 4.** 3D distributed view of aperture-coupled fed microstrip patch antenna.

In this structure, two resonances are provided, one by the patch and the other one by slot. If these two radiators are properly coupled, then the two corresponding resonances become close to each other leading to antenna bandwidth enhancement. The proper coupling between slot and patch can be obtained by tuning the dimensions of slot. By this way, the bandwidth at the order of 20–30% can be obtained. In Ref. [1], a sample is designed for mobile communication base station application with operation frequency of 1.9 GHz, bandwidth of 27% and 9 dBi gain.

In order to increase the bandwidth more, thick dielectric can be used for radiating layer. In this case, the slot size should be increased to make sure that the power is still coupled to the patch properly. In Ref. [3], 40% bandwidth has been reported using this simple technique.

In this technique, the shape and the size of the coupling slot can considerably affect the coupled power and consequently the antenna bandwidth and efficiency. In general, as the coupling power gets stronger by changing the slot shape, thicker substrate for the radiating layer can be used leading to wider impedance bandwidth. On the other hand, as the slot size decreases, the backward radiation which is dominantly caused by the slot decreases enhancing the antenna efficiency. In fact, by choosing the proposer shape for the slot, we try to provide the maximum

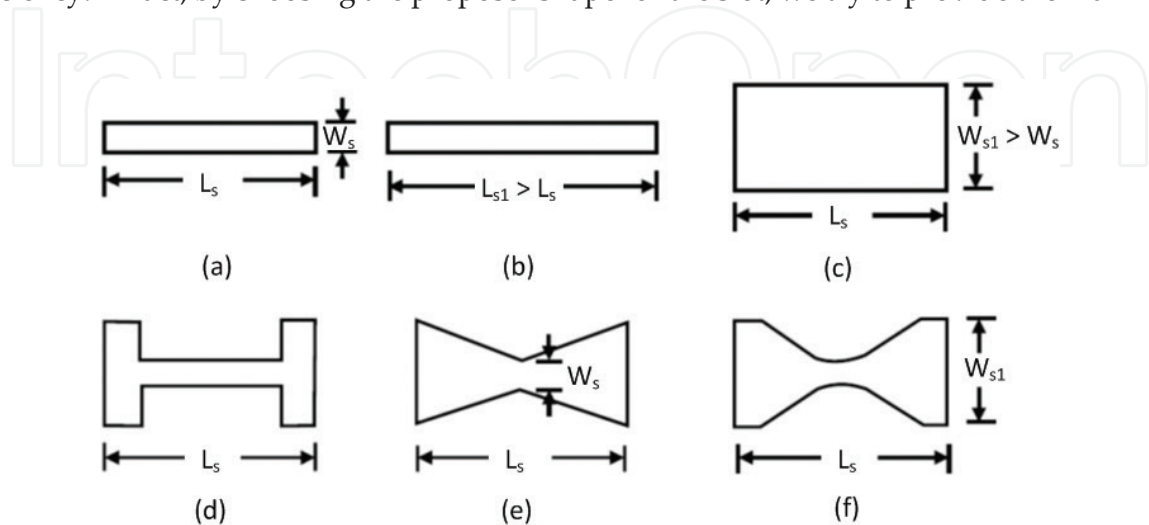


**Figure 5.** Different shapes used for the coupling slot: (a). thin rectangular, (b). longer rectangular, (c). wider rectangular (d). 'H'-shaped, (e). Bowtie-shaped and (f). hourglass-shaped [2, 4].

coupling with the smallest size of the slot. By this way, we can more improve the bandwidth by increasing the radiating layer thickness or reducing its dielectric constant while the maximum efficiency is guaranteed.

One of the most used shapes for the coupling slot is a thin rectangle (**Figure 5(a)**) by which strong coupling can be given with a simple design. However, stronger coupling can be achieved by making it longer or wider (as shown in **Figure 5(b and c)**). The 'H'-shaped and bowtie-shaped slots (**Figure 5(d and e)**) can provide stronger coupling than the rectangular slot since the fields magnitude in rectangular slot has sinusoidal variation; however, in 'H'-shaped and bowtie-shaped slots, it is quite uniform. By combining the 'H'-shaped and bowtie-shaped slots, i.e. making an hourglass-shaped slot shown in **Figure 5(f)**, even more uniform field distribution across the slot and consequently stronger coupling can be achieved [2, 4].

#### 4. Parasitic elements on the single layer

By introducing some dummy elements properly coupled to the driven element at the same radiating layer, i.e. by introducing parasitic patches horizontally coupled to the driven patch, the overall bandwidth of the antenna can be enhanced if the resonant frequency of the coupled elements are slightly different to that of the driven patch since, as shown in **Figure 6**, the overall frequency response is the superposition of the frequency responses of individual patches. In fact, in this technique, both the driven patch and parasitic elements are placed at

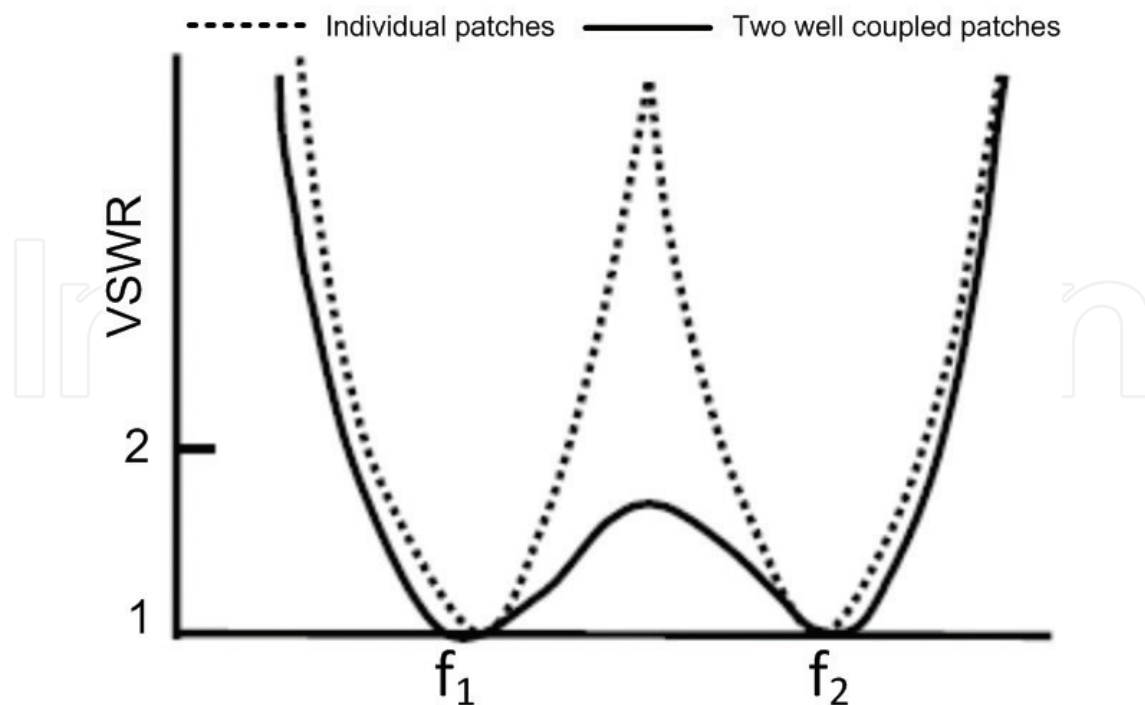


**Figure 6.** Bandwidth enhancement by introducing a dummy patch coupled to the driven patch while the resonance frequencies of the two resonators are quite different [2].

the same layer, meaning that this method is a single layer solution providing easy process for antenna fabrication. The main shortcoming of this method is that the antenna overall size is large leading to the problem of grating lobes for the case, an array is going to develop. In addition, the asymmetry of antenna structure with respect to the centre of driven patch, tends to degrade the radiation pattern. This technique has been realised in four different ways that are described in the following.

#### 4.1. Coupling via radiating edges

In **Figure 7(a)**, a microstrip patch antenna using two unequal parasitic elements at the radiation layer is presented [2, 5]. In the proposed antenna, the driven patch is fed by a probe and two dummy patches are placed at its both sides. In this structure, the parasitic patches are coupled to driven patch via the radiating edges of driven patch. The dimensions of patches are quite different providing three slightly different resonances. The coupling between patches can be tuned by the gaps between them controlling the impedance matching of the antenna.

By this technique, the bandwidth at the order of 20% can be obtained [2]. In **Figure 7(b)**, the frequency response of a sample design presented in Ref. [5] is shown. In this figure, three close well-coupled resonances can be observed which have resulted in antenna bandwidth enhancement. The resulted bandwidth relative to the centre frequency is 10.6% (3.1–3.45 GHz).

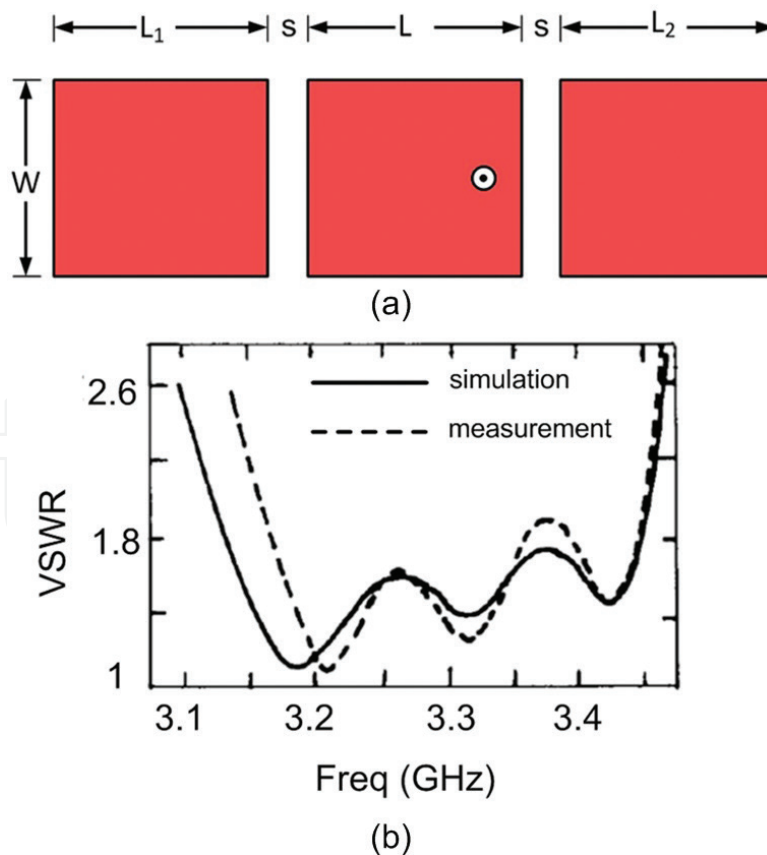


**Figure 7.** Microstrip patch antenna coupled to two parasitic elements at the radiation layer via the radiating edges (a). Antenna topology (b). VSWR plot for a sample designed in Ref. [5].

#### 4.2. Coupling via non-radiating edges

In this method, in the same way as shown in **Figure 7**, two unequal parasitic elements are placed at both sides of the driven patch. But here, as shown in **Figure 8(a)**, the parasitic patches are coupled to driven patch via the non-radiating edges of the driven patch. Since the fields are not uniform at non-radiating edges, unlike at radiating edges where the fields are uniform, the coupling between driven patch and parasitic elements is weaker compared to the previous case where the coupling is provided via radiating edges. So here the gaps between the driven patch and parasitic elements should be smaller than those in the previous case.

By this technique, the bandwidth at the order of 20% can be obtained. In **Figure 8(b)**, the frequency response of a sample design presented in Ref. [2] is shown. In this figure, also three close well coupled resonances can be observed which has resulted in antenna bandwidth enhancement. The resulted bandwidth relative to the centre frequency is 14.5% (2.8–3.3 GHz).

#### 4.3. Coupling via four edges

By mixing the two previous procedures, i.e. placing four patches around the driven patch coupled to it via both radiating and non-radiating edges (as shown in **Figure 9(a)**), further bandwidth enhancement and more gain can be achieved. In Ref. [6], 18.2% bandwidth is obtained using this method. In **Figure 9(b)**, the frequency response of the sample presented in Ref. [6] is shown.

#### 4.4. Annular ring loaded shorted patch

In **Figure 10**, a circular shorted microstrip patch loaded by an annular ring is depicted. In this structure, the driven element is the circular patch which is shorted to the ground plane and the parasitic element is the annular ring surrounding it. The dimensions of both the shorted patch and the ring should be well-determined so that strong coupling between them is formed. Then, by increasing the spacing between them, we can reduce the coupling making it possible to increase the bandwidth. In Ref. [7], a sample of this antenna is designed in which 6.6% bandwidth and 8.4 dBi gain are obtained.

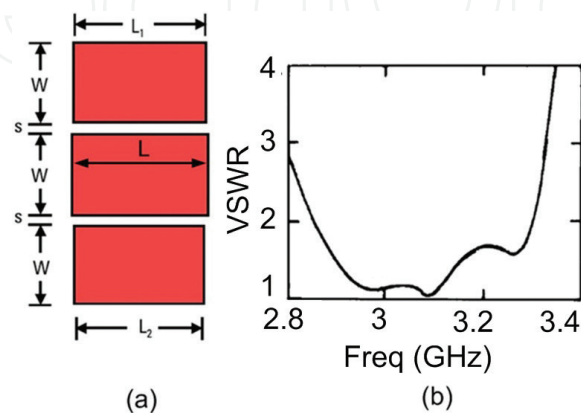
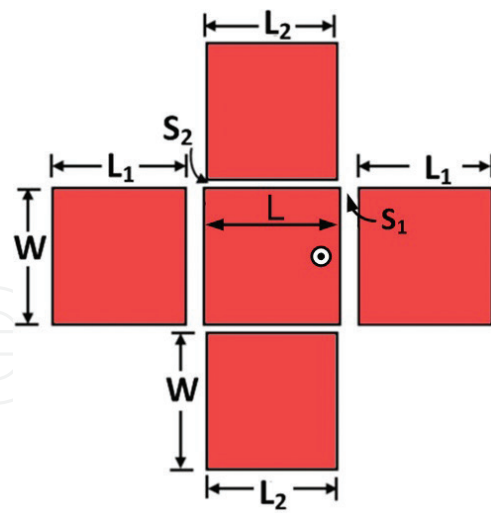
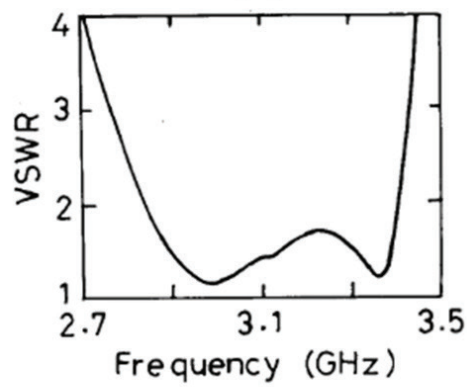


**Figure 8.** Microstrip patch antenna coupled to two parasitic elements at the radiation layer via the non-radiating edges. (a). The configuration of patches and (b). VSWR plot for a sample of antenna presented in Ref. [2].



(a)



(b)

**Figure 9.** Microstrip patch antenna coupled to four parasitic elements at the radiation layer via both radiating and non-radiating edges. (a). The configuration of patches and (b). VSWR plot for a sample of antenna presented in Ref. [6].

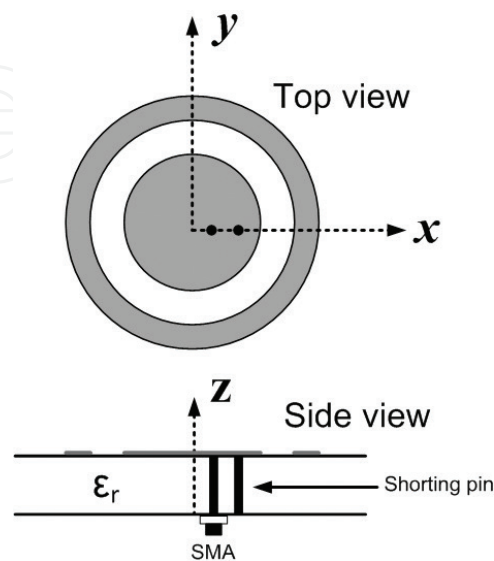


**Figure 10.** Topology of an annular ring loaded shorted patch [7].

## 5. Stacked patches

### 5.1. Configuration

In microstrip patch antennas, the term ‘stacking’ is used for the case where the driven patch is vertically coupled to another patch. By this solution, we do not have the problem of antenna large planar size (which was the issue for the solutions presented in the previous section in which the coupling between parasitic patches and the driven patch were established horizontally) solving the problem of grating lobes when the antenna is used in an array. However, in this technique, since the antenna structure is dual layered, the fabrication process is quite harder than the single-layered antennas presented in previous section. Using this technique, the bandwidth at the order of 20% can be obtained.

In **Figure 11**, a typical probe-fed rectangular stacked patch antenna is shown. It is a dual-layer structure in which the driven patch is located at the lower layer and coupled to the parasitic patch printed on the upper layer. In this configuration, typically rectangular patches are used, however, circular and annular patches can also be used in the same manner. Annular ring (by inner radius) and rectangular (by width) stacked patches have extra degree of freedom compared to circular stacked patches which gives them easier impedance matching control at the expense of slightly reduced bandwidth [1]. In **Figure 12**, the VSWR plot of a sample antenna designed in Ref. [2] using this technique is illustrated. We can see that the bandwidth (VSWR < 2) of 18.8% is obtained.

In the configuration shown in **Figure 11**, there are two resonators, one is the driven patch and the other is the parasitic patch. In design process, the dimensions of patches are chosen so that they resonate at the same frequency. Since two different substrates with different dielectric constants ( $\epsilon_{r1}$ ,  $\epsilon_{r2}$ ) are used, the dimensions of the two patches are different. The mutual coupling between patches shifts the two resonances with respect to each other producing a mutual resonance making it possible to increase the bandwidth. By proper choosing the substrates’ thicknesses and permittivities, the proper coupling between the two resonances

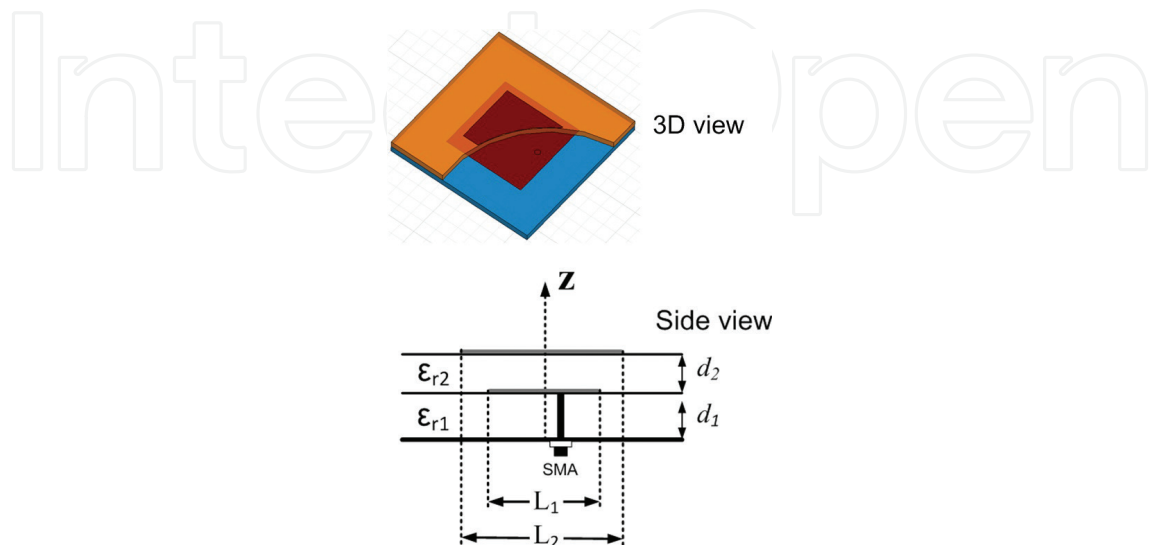


**Figure 11.** The concept of stacking. A rectangular stacked patch.

can be achieved leading to bandwidth enhancement. Broader impedance bandwidth can be obtained by lowering the coupling using high permittivity, say 10, for the lower substrate and low permittivity, say 1, for the upper one [1]. By this way, high surface wave efficiency is also achieved giving the antenna, a better radiation performance.

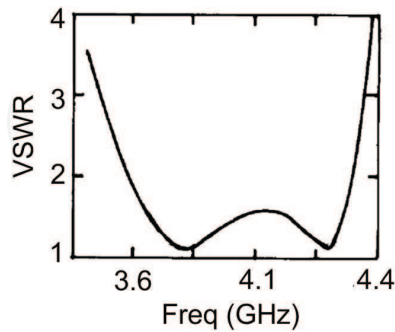


Figure 12. VSWR plot for a sample of antenna presented in Figure 11 [2].

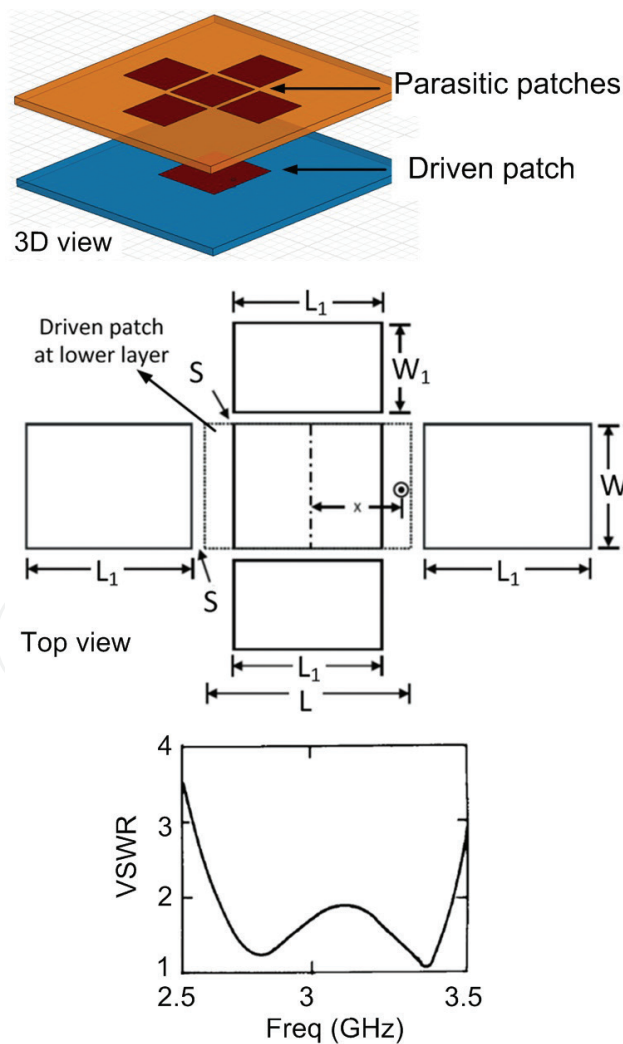
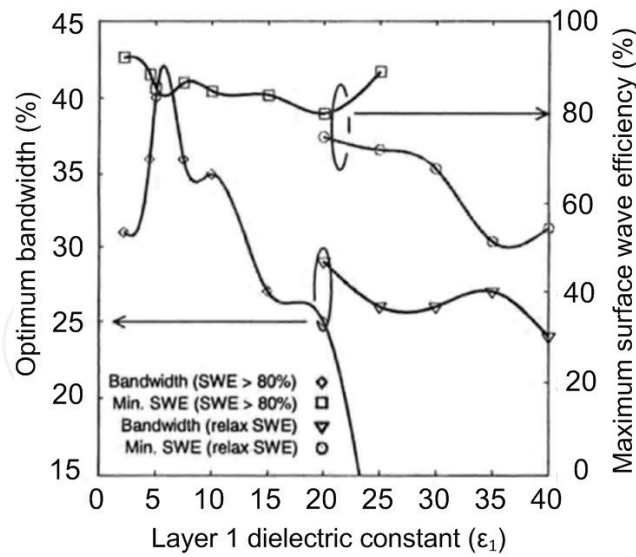


Figure 13. The configuration and frequency response of antenna presented in Ref. [2]. Use of stacking concept for the parasitic elements technique presented in Section 4.



**Figure 14.** Impedance bandwidth and surface wave efficiency (SWE) vs. the lower layer dielectric constant ( $\epsilon_{r1}$ ). The relative permittivity of upper layer is 1.07 [1].

The concept of stacking can also be used for the parasitic elements technique presented in Section 4, placing the driven patch on the lower layer, while the parasitic patches are placed on the upper layer. In Ref. [2], 30% bandwidth could be obtained using one rectangular patch on the bottom layer as the driven path and five parasitic rectangular patches placed on the top layer. **Figure 13** shows the configuration and its frequency response.

## 5.2. Rules of thumb for substrate permittivity

In **Figure 14** [1], the widest impedance bandwidth and minimum surface wave efficiency (SWE) that can be obtained using different laminates for the lower layer while the upper layer uses foam with the relative permittivity of 1.07 as the substrate, are illustrated. It should be noted that the relative permittivity for the upper layer is chosen close to 1 in order to guarantee the maximum surface wave efficiency and bandwidth obtained by tuning  $\epsilon_{r1}$ . We can see that with  $\epsilon_{r1} < 15$ , wide impedance bandwidths (more than 25%) and high efficiency (more than 80%) can be obtained. However, for  $\epsilon_{r1} > 15$ , the surface wave efficiency starts to reduce degrading the radiation performance of the antenna. The reason is that as  $\epsilon_{r1}$  is lower, the surface wave associated with the lower patch is more effectively coupled to the upper patch and consequently to the radiating fields improving the antenna efficiency. As a result, higher  $\epsilon_{r1}$  leads to lower surface wave efficiency.

## 6. Aperture-stacked patches

The aperture-stacked patches are multilayered structures by which the bandwidths at the order of 50–70% can be achieved. **Figure 15** shows the general configuration of an aperture-stacked patch antenna. It consists of  $N$  dielectric layers, two patches and one ground plane

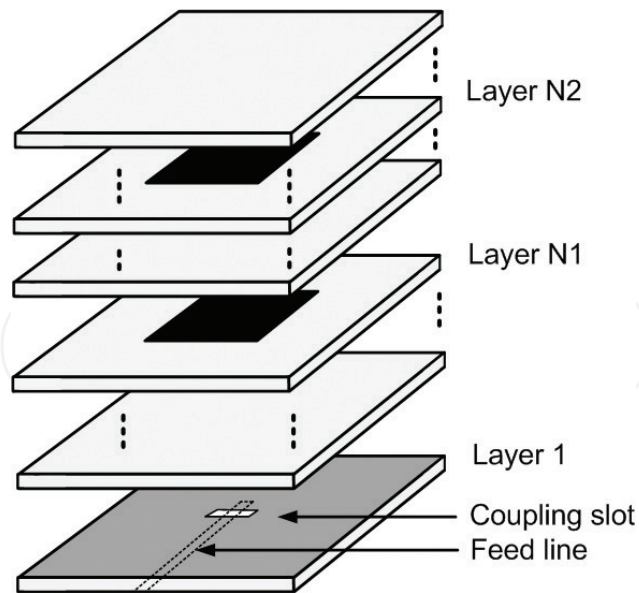


Figure 15. The general configuration of an aperture-stacked patch antenna [1].

at which the coupling aperture, say the slot, is etched. In this configuration, in contrast with the ordinary stacked patches shown in Figure 11, the driven patch (the lower one) is fed indirectly introducing one more coupling mechanism (between feed line and driven patch) which results in wider impedance bandwidth.

In Figure 16, the reflection coefficient,  $S_{11}$ , of a triple layer aperture-stacked patch antenna designed in Ref. [1] for Ka band is presented. It can be observed that the impedance bandwidth of more than 46% relative to centre frequency is obtained. The designed antenna gain is greater than 6 dBi across 26–40 GHz. It should be noted that the presented stacked patch antenna in Ref. [1] is backed by a cavity to increase both front to back ratio and gain.

In Figure 17, an aperture-stacked patch antenna with its geometrical dimensions is shown. In this structure, two offset feed lines are used to excite the slot in order to provide more control

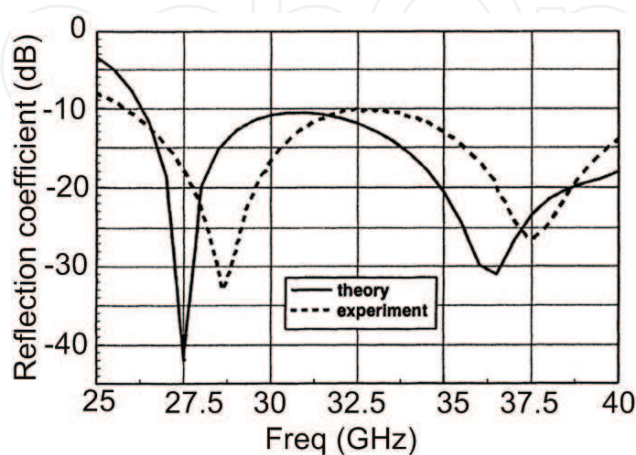


Figure 16. Reflection coefficient of aperture-stacked patch antenna presented in Ref. [1].

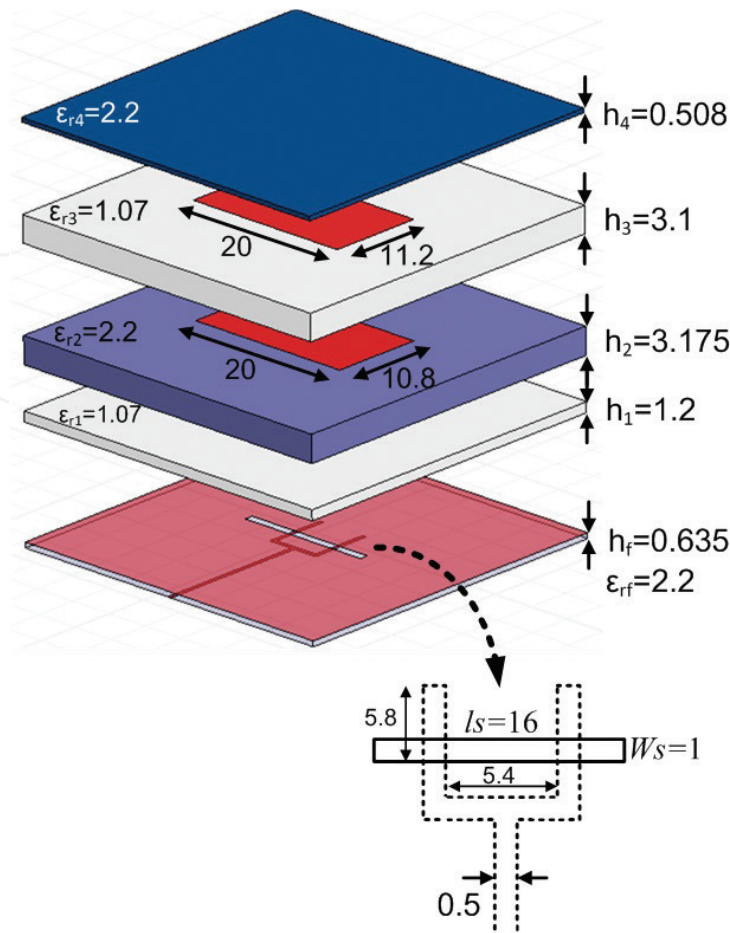


Figure 17. The configuration and dimensions of aperture-stacked patch antenna presented in [1, 8].

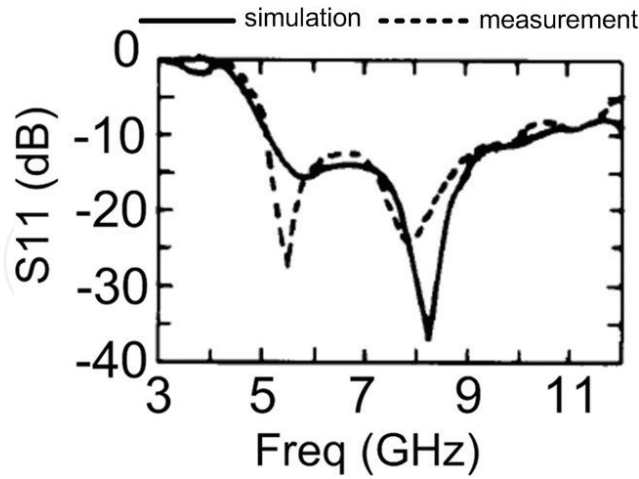


Figure 18. Reflection coefficient of aperture-stacked patch antenna presented in [1, 8].

on coupling power. The two feed lines are  $100\ \Omega$  lines connected to a  $50\ \Omega$  line by a power divider. The reflection coefficient,  $S_{11}$ , of the designed antenna is shown in **Figure 18** [1, 8]. It can be observed that the impedance bandwidth of about 67% relative to centre frequency is obtained. The designed antenna gain is about 7 dBi over its operating bandwidth.

## 7. Broadband techniques for circular polarisation

In previous sections, the broadband techniques for linear polarisation were discussed. However, in many applications such as radar and navigation systems, circular polarisation is required [2]. The axial ratio (AR) bandwidth of conventional microstrip patch antennas is at the order of 1% which is very narrow for many applications. Therefore, some techniques should be applied to increase it. In this section, several configurations that produce wideband circularly polarised radiation are briefly discussed.

### 7.1. Parasitic elements on a single layer

This method uses the same concept used in Section 4 for broadening the bandwidth, however, since here the driven patch is circularly polarised, the AR bandwidth is increased. In **Figure 19** [9, 10], a dual-fed four edged coupled circular polarised microstrip patch antenna is shown. The driven patch is circularly polarised using two orthogonal ports with  $90^\circ$  phase difference. It is coupled to four parasitic patches around it via its four edges. By this way, the two orthogonal modes of the driven patch are coupled to the two orthogonal series of parasitic patches. As a result, the two orthogonal modes are impedance matched in wider frequency band, compared to the case no parasitic patch is used, leading to AR bandwidth enhancement. Since the two orthogonal modes originated by the driven patch have the same amplitude, the gaps between the driven patch and all four parasitic patches should be kept the same in contrast to **Figure 9(a)** where the gaps sizes in the two orthogonal directions have to be different.

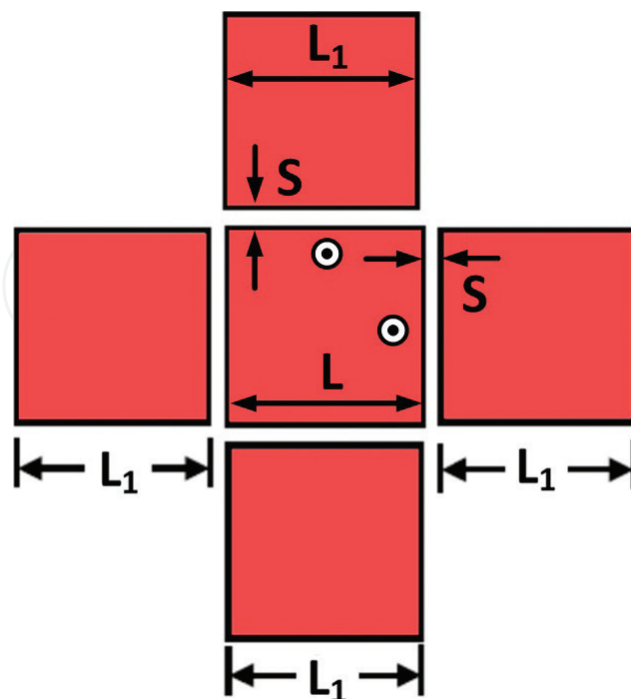


**Figure 19.** Dual-fed four edged coupled circular polarised microstrip patch antenna [9, 10].

It should be noted that here, in order to keep the amplitude of orthogonal radiating modes well balanced to improve gain, bandwidth and AR, all parasitic patches should be identical keeping the same shapes and the same sizes. Since the driven patch is square shaped, the parasitic patches also should be square shaped as well. By this single-layer technique, the AR bandwidth at the order of 10% can be achieved.

## 7.2. Stacking

Here, also in the same way as described in Section 5, the AR bandwidth can be enhanced using stacking technique. In **Figure 20**, a circular polarised dual-fed stacked microstrip patch is shown. The driven patch is dual-fed and produces circular polarisation. The two orthogonal modes generated by the driven patch are vertically coupled to the parasitic patch and excite two orthogonal modes inside it. In this case, we can say the two orthogonal modes of lower patch are coupled to the two orthogonal modes of upper one. As a result, these two orthogonal modes are impedance matched over wider frequency band compared to the case no parasitic patch is used leading to wider AR bandwidth. In Ref. [11], a sample antenna base on the configuration shown in **Figure 20** is designed and 18% AR bandwidth is obtained. In Ref. [11], both the driven and parasitic patches are squared.

## 7.3. Aperture coupling

By changing the slot/patch shape in the aperture coupling technique discussed in Section 3.2, circular polarised radiation with enhanced AR bandwidth can be achieved [12–17]. In **Figure 21**, an aperture-coupled square patch antenna with cross-shaped coupling slot is shown. By this

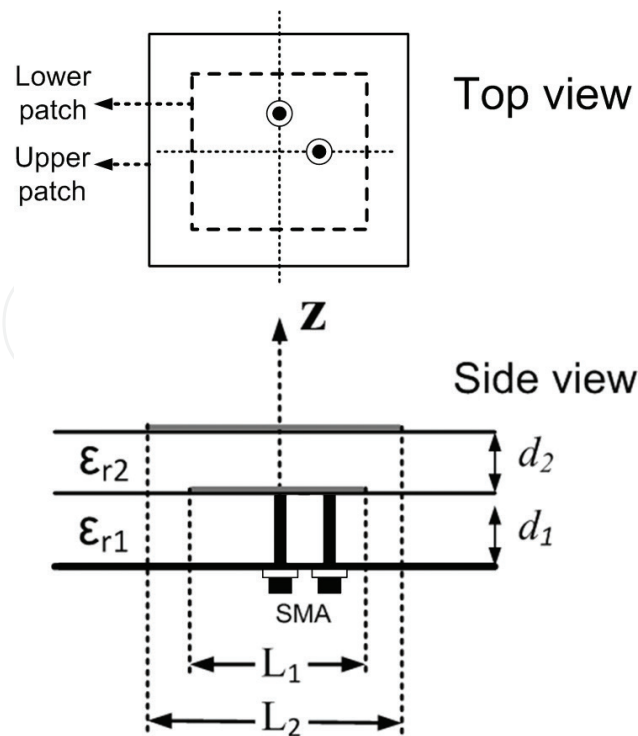


**Figure 20.** AR bandwidth enhancement by stacking technique.

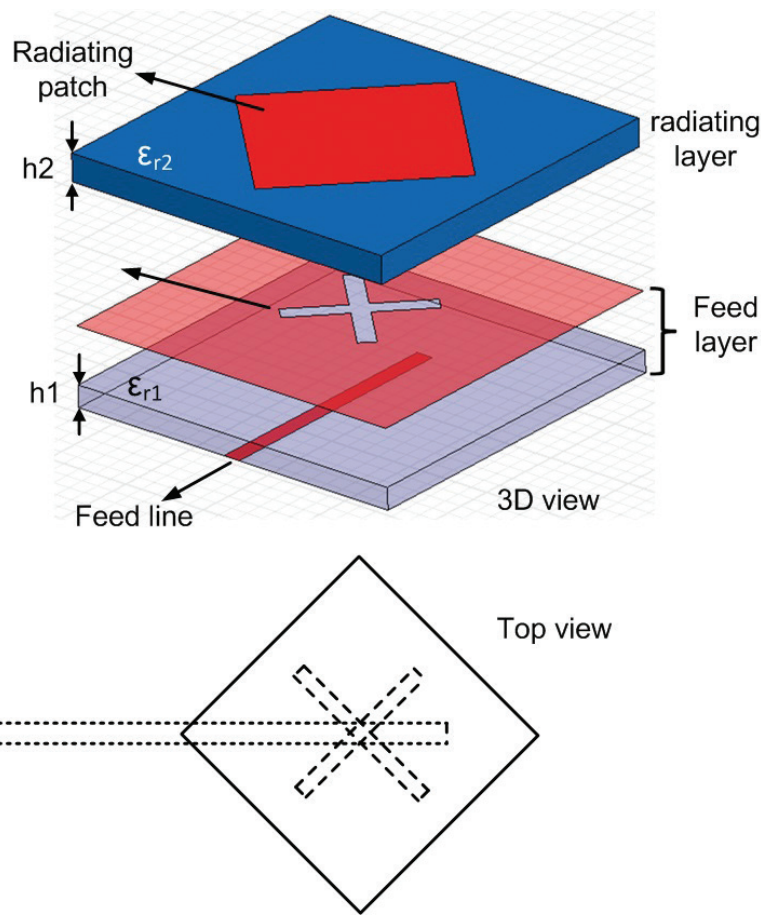


**Figure 21.** Aperture-coupled microstrip patch antenna using cross-shaped coupling slot. Different lengths are chosen for the two crossed slots to provide 90° phase difference between the two orthogonal modes.

configuration, two orthogonal modes originated by the cross-shaped slot are coupled to the two orthogonal modes of the patch leading to bandwidth enhancement of each mode and consequently expansion of AR bandwidth. In Ref. [12], a sample antenna is designed using the configuration shown in **Figure 21** and 1.4% AR bandwidth is obtained.

In **Figure 21**, two crossed slots and a square patch were used. However, the same performance can be obtained using a single slot and modifying the patch shape. In **Figure 22**, an aperture-coupled patch antenna using a single 45° rotated slot and a nearly square patch are depicted. In Ref. [17], a circular polarised antenna with AR bandwidth of about 1.1% is designed using this configuration.

#### 7.4. Array

Probably the widest AR responses can be obtained using the array technique. In this method, the elements of array are sequentially rotated while fed by equal magnitudes and different phases. The elements are either linear polarised or circular polarised, however, the whole array provides circular polarisation. In **Figures 23** and **24** [18–21], several array configurations for providing wideband circular polarised radiation are shown. In these figures, the array elements are circular polarised.

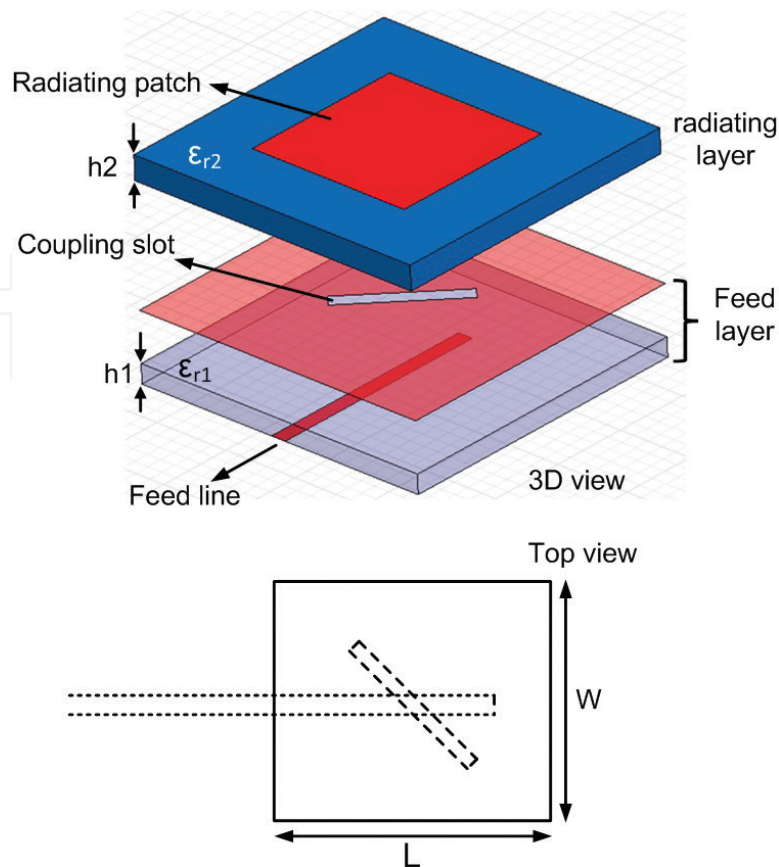


Figure 22. Aperture-coupled patch antenna using a single  $45^\circ$  rotated slot and a nearly square patch.

Figure 23(a) [18] shows a  $1 \times 2$  array in which the elements are  $90^\circ$  out of phase and  $90^\circ$  rotated relative to each other. The  $90^\circ$  phase difference is provided by applying additional length to the feed line. In Figure 23(b) [19], a  $2 \times 2$  array using the same concept is shown. In this figure, each element has  $90^\circ$  rotation and  $90^\circ$  phase difference relative to its neighbouring element. In Figure 24(a) [20], a  $2 \times 4$  array is illustrated in which the phase of each element is equal to its rotation angle relative to the element fed by  $0^\circ$  phase. A sample of this configuration is designed in

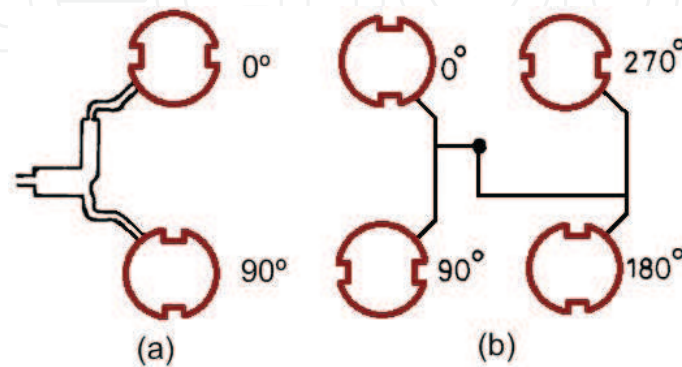
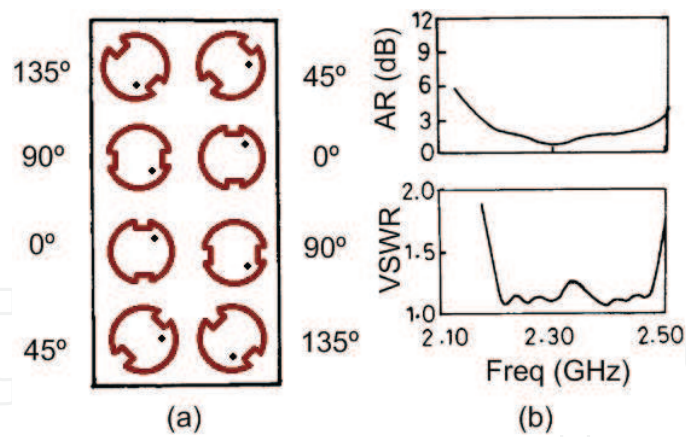


Figure 23. Two sequentially rotated array configurations using circular polarised elements. (a). A  $1 \times 2$  array with  $90^\circ$  rotated and phase-shifted elements. (b). A  $2 \times 2$  array in which each element has  $90^\circ$  rotation and phase difference relative to its neighbouring element [18, 19].



**Figure 24.** A sample  $2 \times 4$  sequentially rotated array. (a). Antenna configuration and (b). VSWR and AR of designed antenna vs. frequency [20].

Ref. [20] and its frequency responses including VSWR and AR are shown in **Figure 24(b)**. It can be observed that the bandwidth for  $VSWR < 1.5$  is 13.7% and the bandwidth for  $AR < 3$  is 14%.

In the configurations shown in **Figures 23** and **24**, the array elements are in direct contact with feed network. However, non-contact feeding techniques such as proximity coupled and aperture-coupled feedings can also be applied here [21].

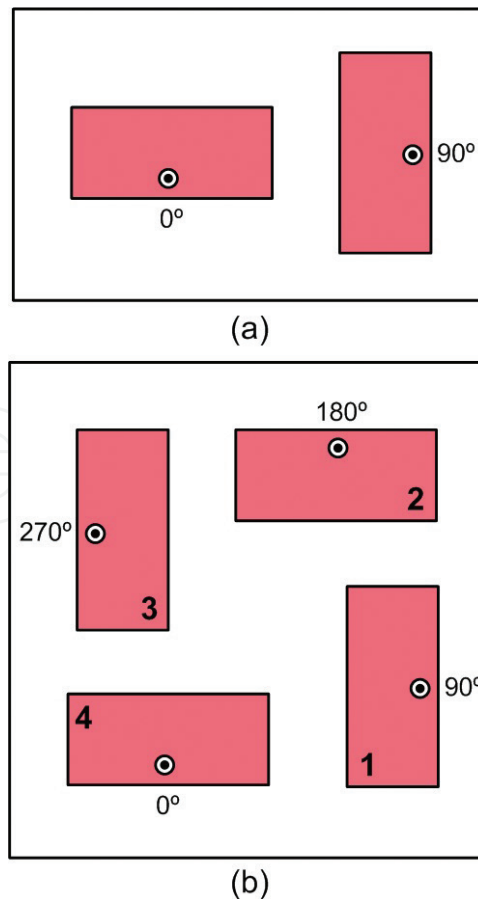


**Figure 25.** Two sample sequentially rotated arrays using linear polarised elements: (a). a  $1 \times 2$  array and (b) a  $2 \times 2$  array [22].

As mentioned before, wideband circular polarisation using sequentially rotated array can also be achieved using linear polarised elements. In **Figure 25**, two sample arrays are shown [22]. The arrangement of elements is exactly the same as that shown in **Figure 23**. **Figure 25(a)** shows a  $1 \times 2$  array with two linear polarised orthogonal patches fed by  $90^\circ$  phase difference. It is easy to understand that by this configuration, two orthogonal modes with  $90^\circ$  phase difference are radiated by the two patches resulting in circular polarised radiation. In **Figure 25(b)**, a  $2 \times 2$  sequentially rotated array is shown. In this arrangement, there exists two set of orthogonal patches (patches 1 and 3 and patches 2 and 4) that generate the two orthogonal modes with  $90^\circ$  phase difference leading to gain enhancement compared to the antenna shown in **Figure 25(a)**.

In order to increase the gain more, the number of elements should be increased. In Ref. [23], it is shown that for this purpose, if  $N$  elements are to be used, then they should be arranged in a circular ring and the rotation angle of each element relative to its neighbouring element should be  $360/N$  degree. Furthermore, the phase shifting between the neighbouring elements should be  $360/N$  as well.

## 8. Other techniques

In this section, some other techniques that are reported in the literature are introduced and briefly described. However, as we know there exist numerous works on bandwidth enhancement of microstrip patch antennas, with respect to all researchers who have worked on this issue, we have selected a few number of works and presented here.

### 8.1. Log-periodic array of patches

In [24–26], the idea of log-periodic antennas for providing very wide bandwidths has been applied to microstrip patches. In this technique, the microstrip patches are arranged in a log-periodic formation. The patches are series fed by a microstrip line either directly or indirectly. In **Figure 26(a and b)**, both direct- and indirect-fed configurations are illustrated. In the configuration shown in **Figure 26(a)**, each patch is coupled to the feed line located at the lower layer; however in **Figure 26(b)**, each patch is directly connected to feed line via a quarter-wave transformer for easier impedance matching (i.e. the length 'd' is chosen  $\lambda/4$  where  $\lambda$  is the wavelength corresponding to the resonance frequency of the patch). In **Figure 26(c)**, the VSWR plot of a sample antenna designed in Ref. [26] based on the configuration shown in **Figure 26(b)**, is shown. It can be observed that very wide bandwidth (about 100%) is obtained by making use of this configuration.

The radiation pattern of antennas shown in **Figure 26** is broadside, unlike the conventional log-periodic dipole array which radiates at end-fire direction. Although by using log-periodic configuration, very wide bandwidths can be achieved, but the main beam direction scans vs. frequency makes it impossible to provide constant beam direction through the whole bandwidth.

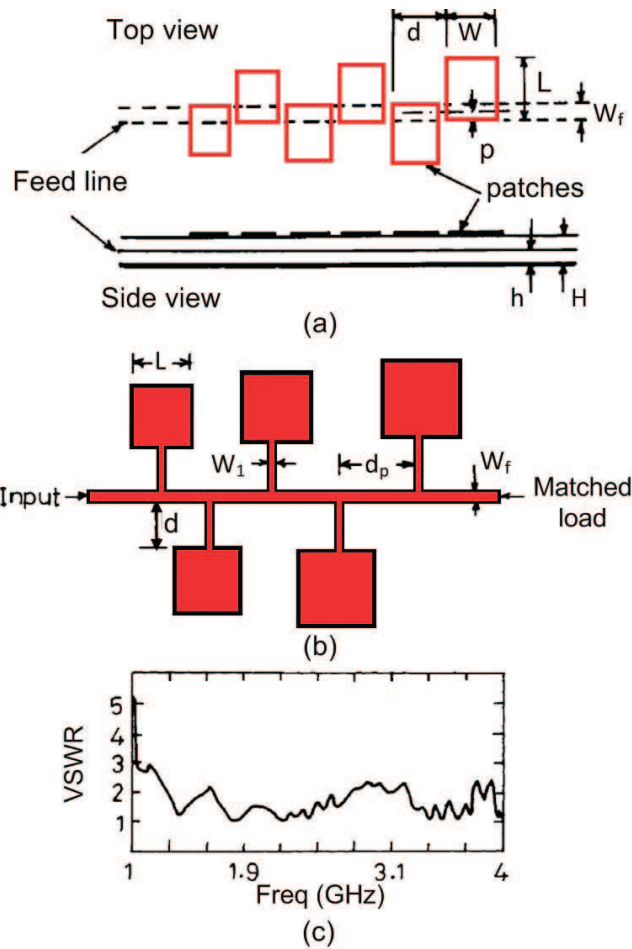


**Figure 26.** Microstrip patches arranged in log-periodic array formation. (a). Indirect feeding, (b). direct feeding and (c). VSWR plot of a sample antenna designed in Ref. [26] based on the configuration shown in Figure 29(b).

## 8.2. E-shaped patch

In Ref. [27], an E-shaped patch backed by a SIW<sup>1</sup> cavity is proposed by which 10.9% bandwidth could be obtained. The antenna structure is illustrated in Figure 27. As shown, the radiating element is an E-shaped patch backed by SIW cavity and fed by a strip line which is loaded by some stubs. Direct contact between feed line and radiating patch is provided by a metalized via at the centre performing like a probe.

In Ref. [28], it is declared that for a conventional E-shaped patch (i.e. a single layered E-shaped patch antenna fed by a simple probe) in order to provide impedance matching for the lower resonating mode, we need to choose the substrate thickness more than  $0.07\lambda$ , since the inductance contributed by the probe is very low and the capacitance introduced by the patch and ground becomes very large [27]. In this design, some stubs are introduced at the end of strip line in order to provide more inductance and make it possible to impedance match the lower resonating mode even with thin substrates of  $<0.07\lambda$  thicknesses.

<sup>1</sup>Substrate integrated waveguide.

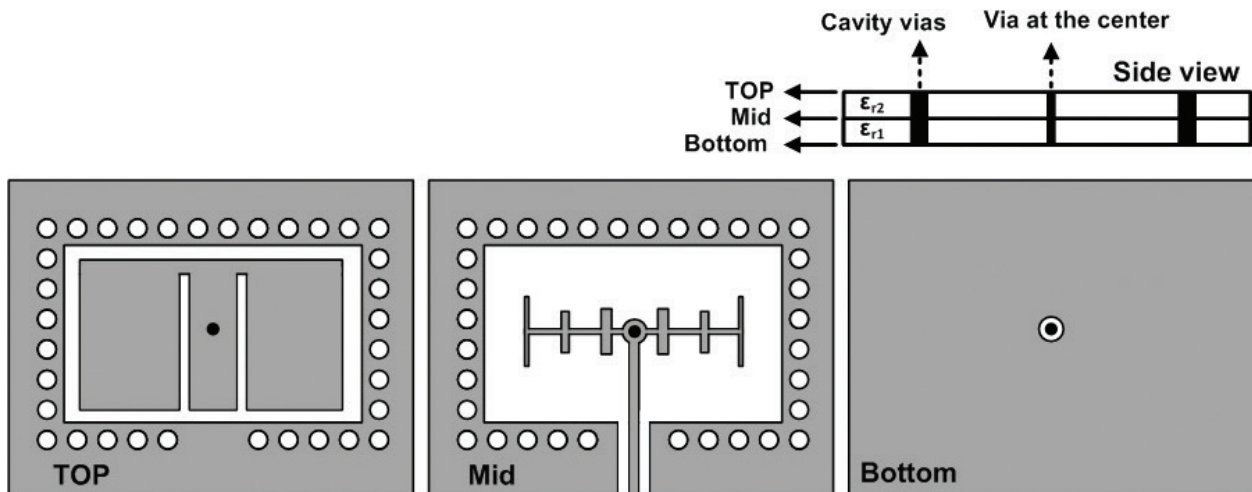


Figure 27. The E-shaped patch antenna configuration presented in Ref. [27].

The input impedance and current distributions corresponding to the two resonating modes of radiating patch for the two cases, with and without stubs, are depicted in **Figure 28**. It can be clearly observed that if the stubs are not used, the lower resonating frequency cannot be created with the thin substrate used in this design. However, by applying the stubs and fine tuning of their dimensions, two resonating modes that are successfully impedance matched make it possible to increase the impedance bandwidth. In **Figure 29**, the reflection coefficient,  $S_{11}$ , of the antenna designed in Ref. [27] is shown and the impedance bandwidth ( $S_{11} < -10$  dB) of 10.9% (9.45–10.54 GHz) can be observed.

### 8.3. L-shaped feeding

In [29, 30], an L-shaped probe is used to feed a microstrip patch and demonstrated that by this way, the impedance bandwidth can be increased. This method can be interpolated as a

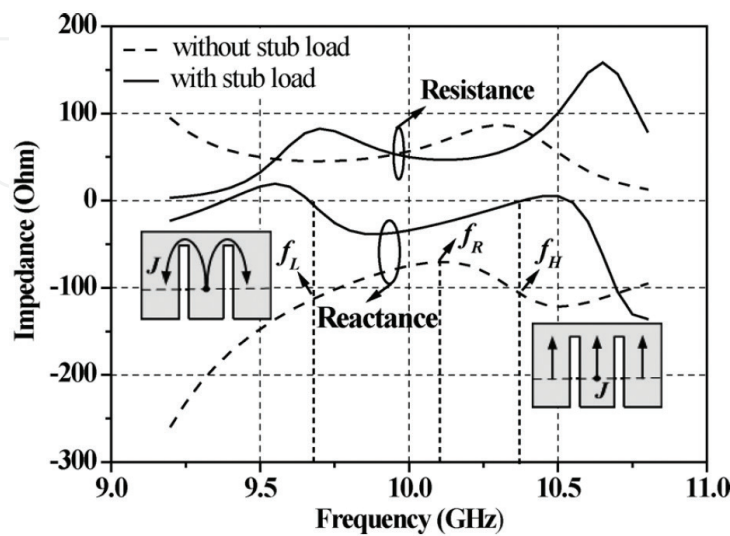
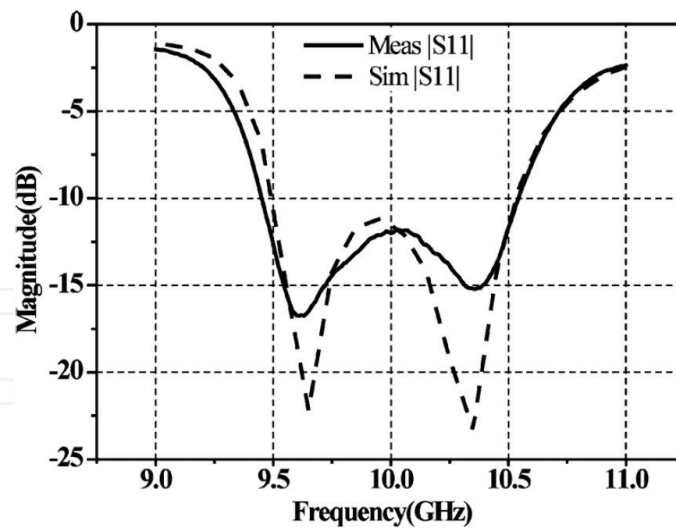


Figure 28. The input impedance and current distributions corresponding to the two resonating modes of radiating patch for the two cases, with and without stubs, for the antenna shown in **Figure 27** [27].



**Figure 29.** Reflection coefficient,  $S_{11}$ , of the sample antenna designed in Ref. [27] based on the configuration shown in Figure 27 [27].

combination of proximity coupled feeding and stacking technique. In **Figure 30**, a rectangular patch antenna fed by an L-shaped probe is illustrated. As shown, the L-shape probe is realised by connecting a metalized via to the feed line. In this figure, the L-shaped probe is fed by a strip line in order to suppress parasitic radiation due to the feed structure. The simulated  $S_{11}$  of a sample designed in Ref. [30] is shown in **Figure 31**. It can be seen that 50.4% (46–77 GHz) impedance bandwidth is achieved.

#### 8.4. Microstrip monopole slotted antenna

In Ref. [31], a microstrip monopole slotted antenna is introduced and its performance using three different shapes (straight, L and inverted-T) for the slot is investigated and it is shown

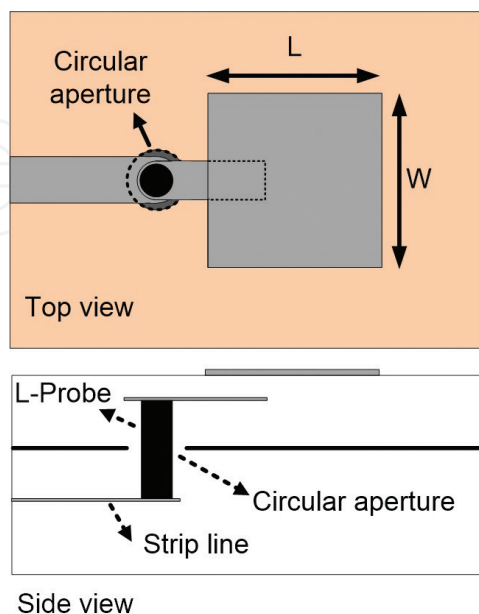


**Figure 30.** Rectangular patch antenna fed by an L-shaped probe [30].

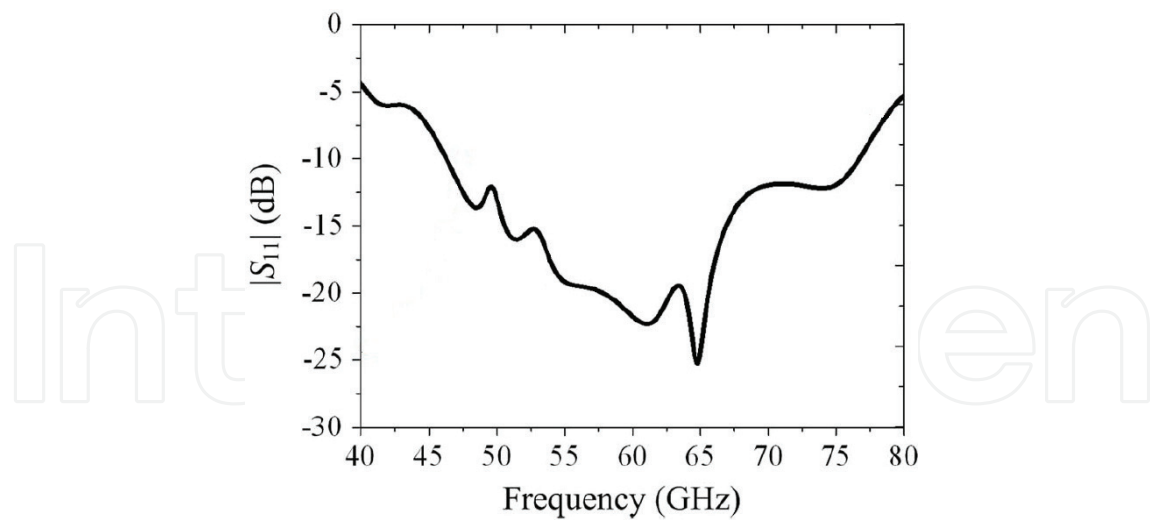


**Figure 31.** The simulated  $S_{11}$  of a sample antenna designed in Ref. [30] based on the configuration shown in **Figure 30**.

that by making use of this single-layer configuration, a wide impedance bandwidth of more than 80% can be achieved. It should be said that this antenna has omnidirectional radiation pattern and consequently lower gain compared to the antennas presented in previous sections.

In **Figure 32**, the antenna configuration for three different slot shapes is shown. As depicted, it is a single-layer structure in which the slot is electromagnetically coupled to the feed line. The presence of slot introduces additional resonances that can be well-coupled to the patch resonance leading to antenna bandwidth enhancement.

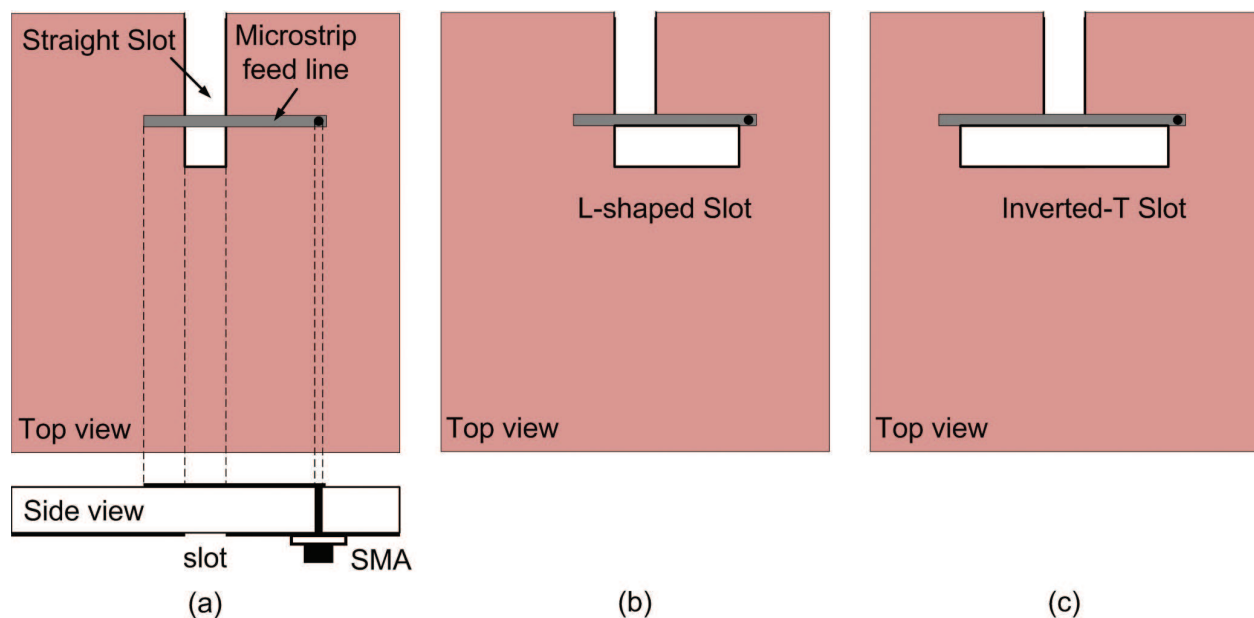


**Figure 32.** Microstrip monopole slotted antenna with three different slot shapes: (a). straight slot, (b). L-shaped slot and (c). inverted-T slot [31].

In Ref. [31], three samples of antennas shown in **Figure 32** are designed. **Figure 33** shows the reflection coefficients,  $S_{11}$ , of the designed antennas. It can be clearly observed that for the case a single straight slot is used (**Figure 32(a)**), one additional resonance is created resulting in 57% bandwidth (2.5–4.5 GHz); however, for the cases where L-shaped (**Figure 32(b)**) or inverted-T slot (**Figure 32(c)**) is used, three additional resonances are created resulting in wider impedance bandwidth: 82% (2.42–5.78 GHz) for the former and 80% (2.74–6.4 GHz) for the latter. The reason is that for the cases of L-shaped and inverted-T slots, the two orthogonal arms of slot perform as two separate resonators properly coupled to each other and the patch making four well-coupled resonances which leads to significant enhancement of the bandwidth.

### 8.5. Defected ground/patch

Defecting the patch/ground has been used as a technique to improve the radiation characteristics of microstrip patch antennas. Mutual coupling suppression in arrays [32–34], improving the efficiency [35], reducing the antenna size [36] and lowering the cross-polar level [37–39] and Bandwidth enhancement [40–42] are some examples of this. Here, our focus is on the latter one, i.e. the bandwidth enhancement.

In Ref. [40], a double U-shaped slot is introduced to the ground plane of a microstrip monopole antenna in order to enhance its impedance bandwidth. With the resultant structure, the impedance bandwidth of 114% was obtained. The proposed structure and reflection coefficient  $S_{11}$  of a designed sample in Ref. [40] are illustrated in **Figure 34**.

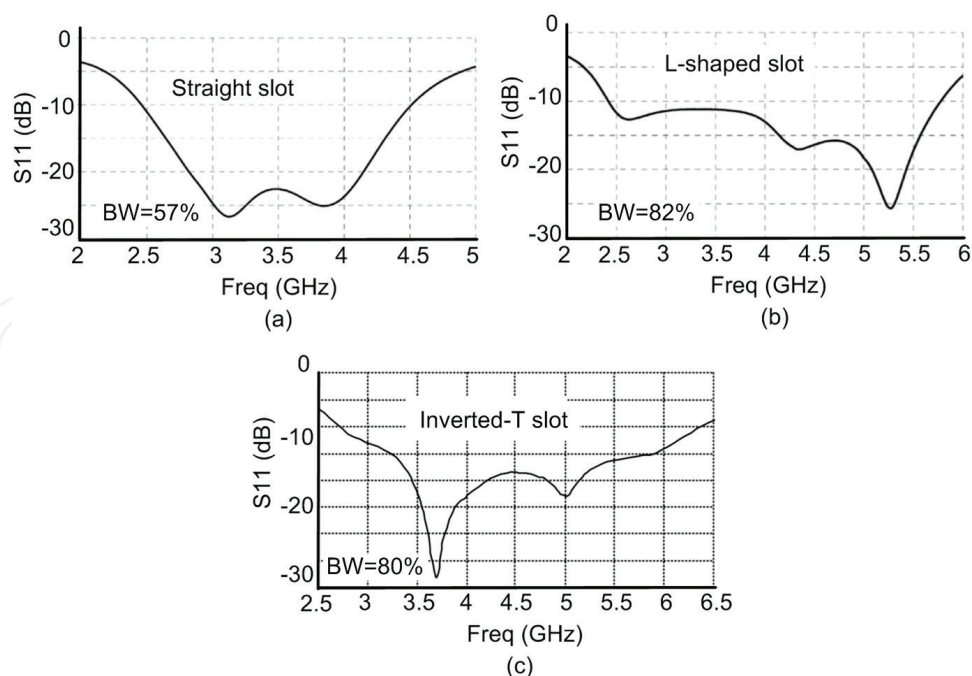


**Figure 33.** The reflection coefficients,  $S_{11}$ , of the sample antennas designed in Ref. [31] based on the configurations shown in **Figure 32**. (a). Straight slot, (b). L-shaped slot and (c). inverted-T slot [31].

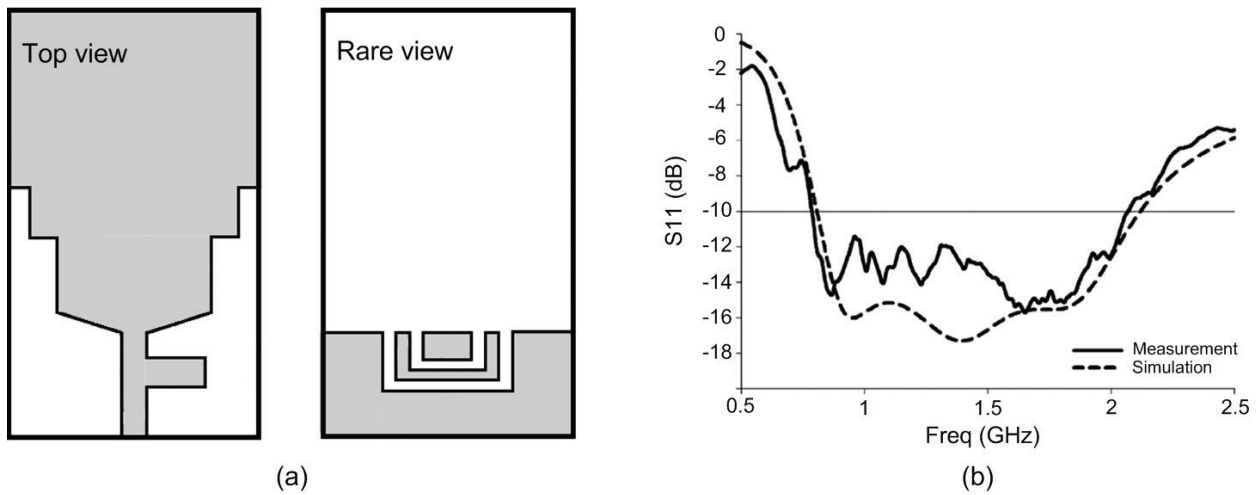


**Figure 34.** The proposed defected ground microstrip monopole antenna presented in Ref. [40]. (a). Topology of the structure. (b). Reflection coefficient  $S_{11}$  of a designed sample in Ref. [40].

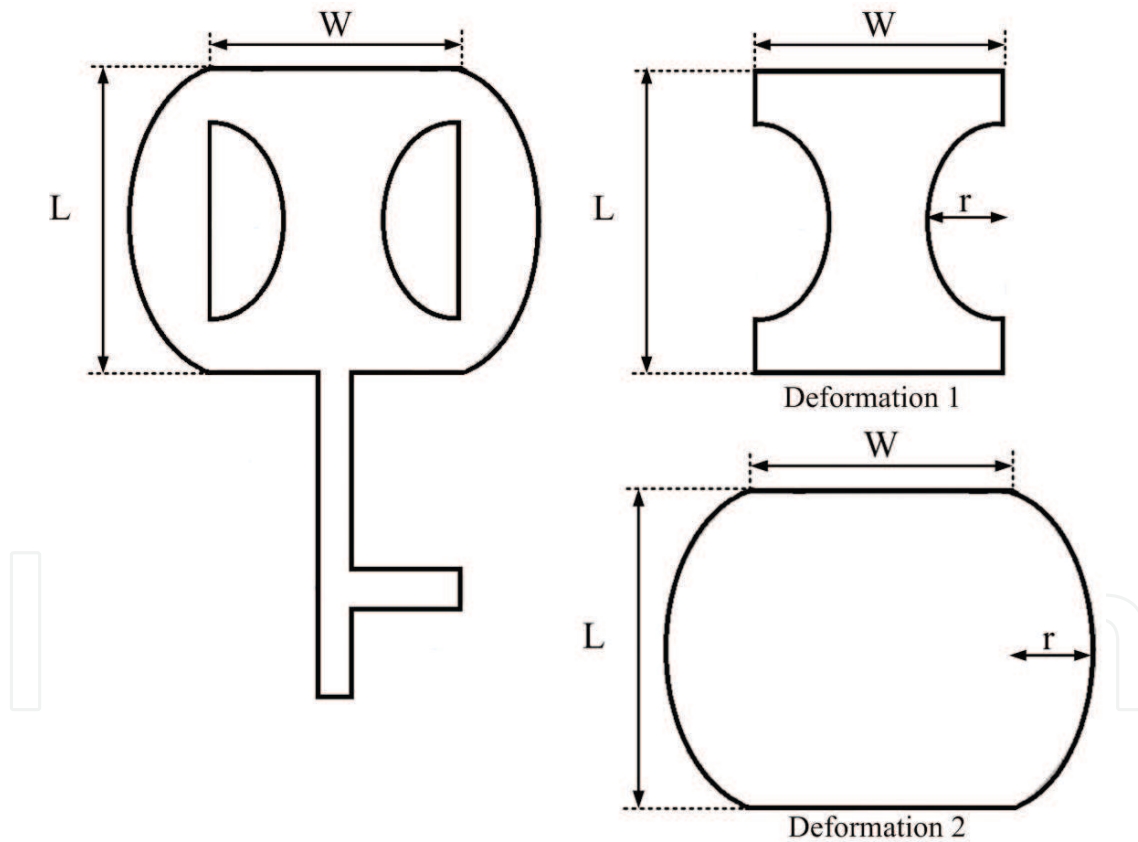


**Figure 35.** The proposed D-shaped defected microstrip patch presented in Ref. [41]. Complete structure and two deformations used in it [41].

In Ref. [41], a D-shaped defected patch is used for bandwidth enhancement. The proposed structure and the two deformations used in it are shown in **Figure 35**. By deformation 1, the resonant frequency of  $TM_{10}$  mode decreases since the effective length of the patch increases for this resonating mode. However, the deformation 2 performs inversely, i.e. it decreases the

effective length of the patch for  $TM_{10}$  mode increasing its resonant frequency. As a result, combination of these two deformations makes a D-shaped defected patch which can produce two resonant frequencies by the two effective lengths of inside and outside of D-shaped defection. The open circuit stub connected to the feed line is used for impedance matching.

In **Figure 36**, a fabricated sample of proposed structure and its reflection coefficient  $S_{11}$  are depicted. The reflection coefficient of the proposed structure is also compared with that of a conventional patch and 5% bandwidth enhancement can be observed in the measurement result.

In Ref. [42], a dumbbell-shaped defected patch is used to both increase the bandwidth and enhance polarisation purity. The proposed structure is shown in **Figure 37**. As shown, a pair of thin slots (with the dimensions  $l_1 \times S_{w1}$ ) is etched near the non-radiating edges and four wider slots (with the dimensions  $l_2 \times d_w$ ) are positioned near the patch corners. By this way, the fields corresponding to non-radiating edges and corners which mainly contribute to cross-polar radiation are perturbed leading to more pure radiations. In Ref. [42], it is shown that each  $l_1 \times S_{w1}$  slot introduces a reactance parallel to the input impedance of the patch in such a way that the variation of patch input reactance vs. frequency (as shown in **Figure 38**) becomes smaller compared to the conventional patch. This fact may point to the broader bandwidth of the proposed structure relative to the conventional patch.

In **Figure 39**, the reflection coefficient of a sample antenna designed in Ref. [42] is illustrated and compared with that of a conventional patch. Results show that the proposed antenna produces broader bandwidth. The measurement result shows 16% bandwidth for the designed sample.

### 8.6. Recent works

In this part, we have tried to provide a brief review of the most important works that has been done in recent years to give the reader a prospective of the latest researches on bandwidth enhancement of microstrip patch antennas.

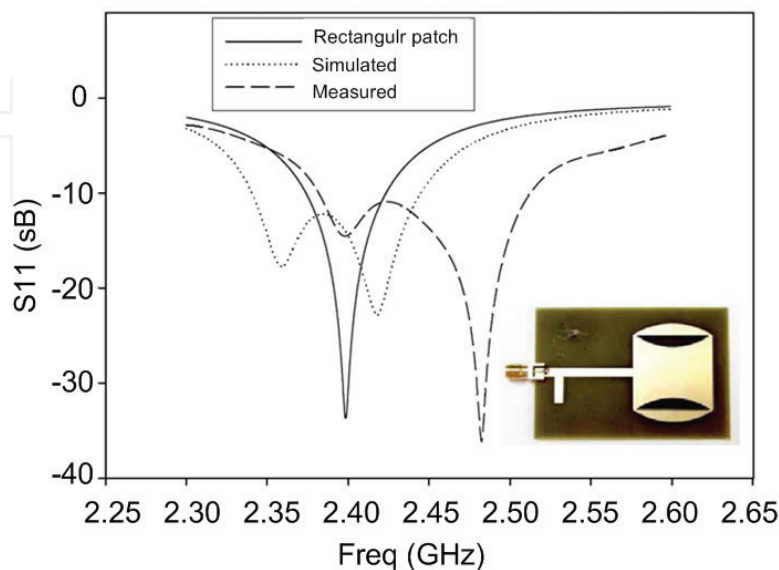


**Figure 36.** Fabricated sample of D-shaped defected microstrip patch presented in Ref. [41] and comparison of its reflection coefficient with that of a conventional patch.

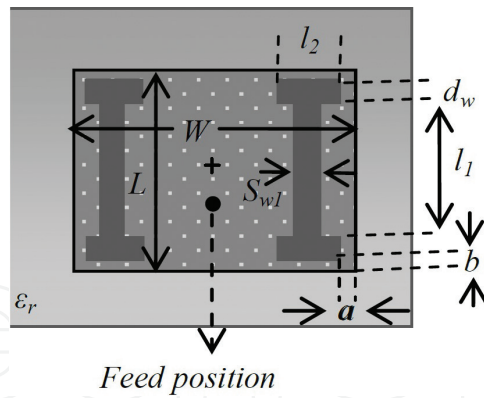


**Figure 37.** The proposed dumbbell-shaped defected patch presented in Ref. [42].

The latest works focused on the enhancement of the bandwidth without increasing the size and height of antenna [43–46]. In [43–45], differential feeding is used to suppress the excitation of undesired modes. Then by joining the desired modes (or by introducing extra modes between the desired modes), the bandwidth for broadside radiation is enhanced.

In Ref. [43], by differential feeding for a rectangular patch, the unwanted modes  $TM_{20}$ ,  $TM_{12}$  and  $TM_{22}$  are suppressed and the favourite broadside modes  $TM_{10}$  and  $TM_{30}$  are excited. Then by making use of two stubs connected to the radiating edges of the patch and a stepped ground plane, as shown in **Figure 40(a)**, it became possible to enclose the desired modes leading to bandwidth enhancement. In **Figure 40(b)**, the reflection coefficient of a sample designed in Ref. [43] is shown and about 10% bandwidth is observed.

In Ref. [44], as shown in **Figure 41(a)**, a differentially fed equilateral triangular patch is loaded by shorting posts. In this structure, the desired modes  $TM_{10}$  and  $TM_{11}$  are well excited using differential feeding. Loading the patch with shorting pins generates additional mode, i.e. zero mode, between the two favourite modes which makes it possible to enhance the antenna

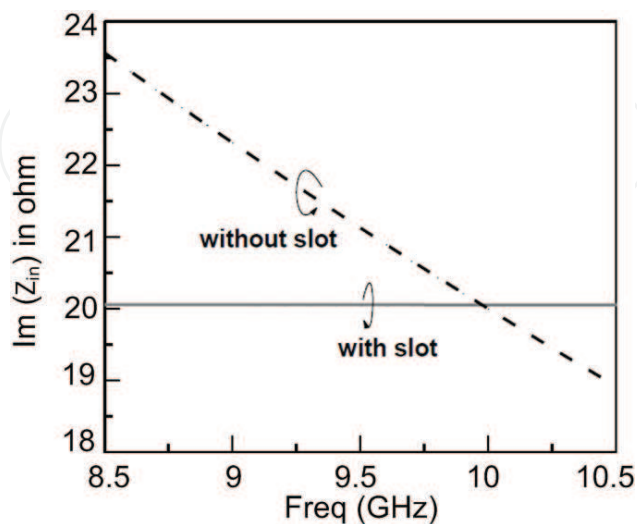


**Figure 38.** Variation input reactance of proposed patch in Ref. [42] vs. frequency and its comparison with that of a conventional patch.

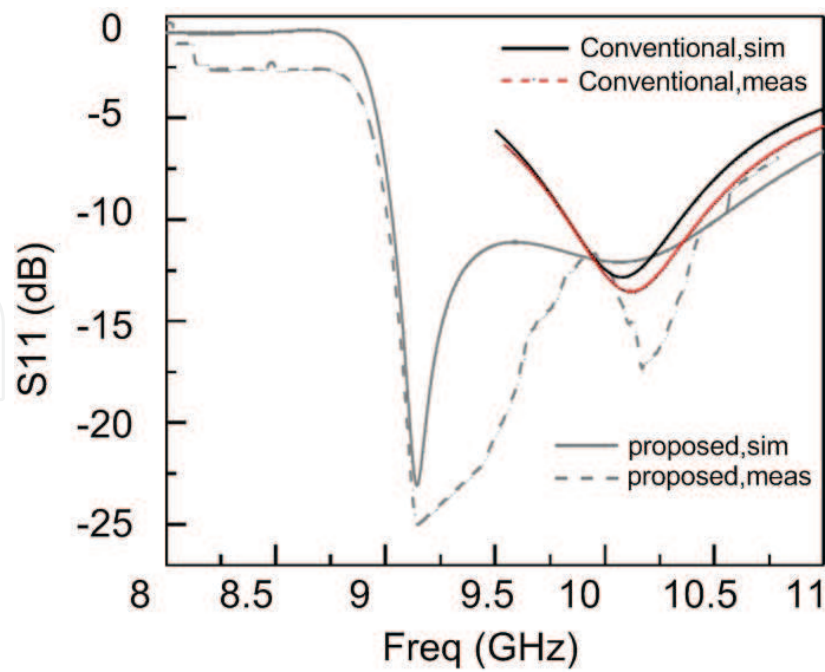


**Figure 39.** Reflection coefficient of a sample antenna designed in Ref. [42] and its comparison with that of a conventional patch.

bandwidth by making a proper coupling between the three modes. It should be noted that the shorting pins are located so that they do not perturb the field distribution of  $TM_{10}$  and  $TM_{11}$  modes and consequently do not affect them. In **Figure 41(b)**, the reflection coefficient of a sample antenna designed in Ref. [44] is shown and it is observed that more than 50% bandwidth could be obtained.

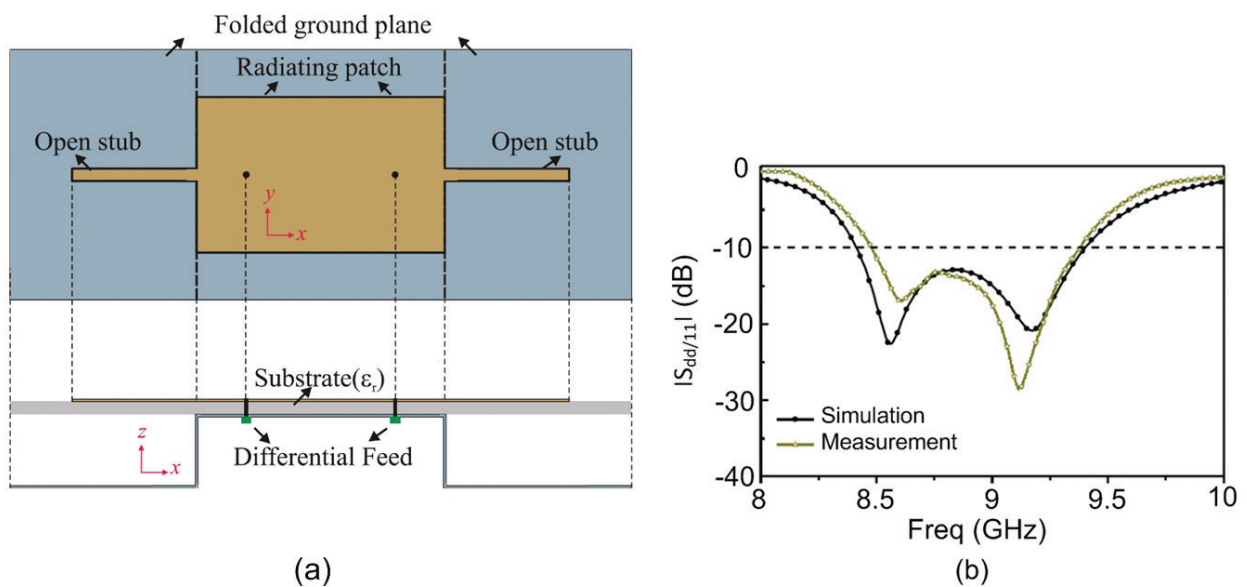


**Figure 40.** The differentially fed rectangular patch antenna presented in Ref. [43]. (a). Topology of the structure. (b). Reflection coefficient of a sample designed in Ref. [43].

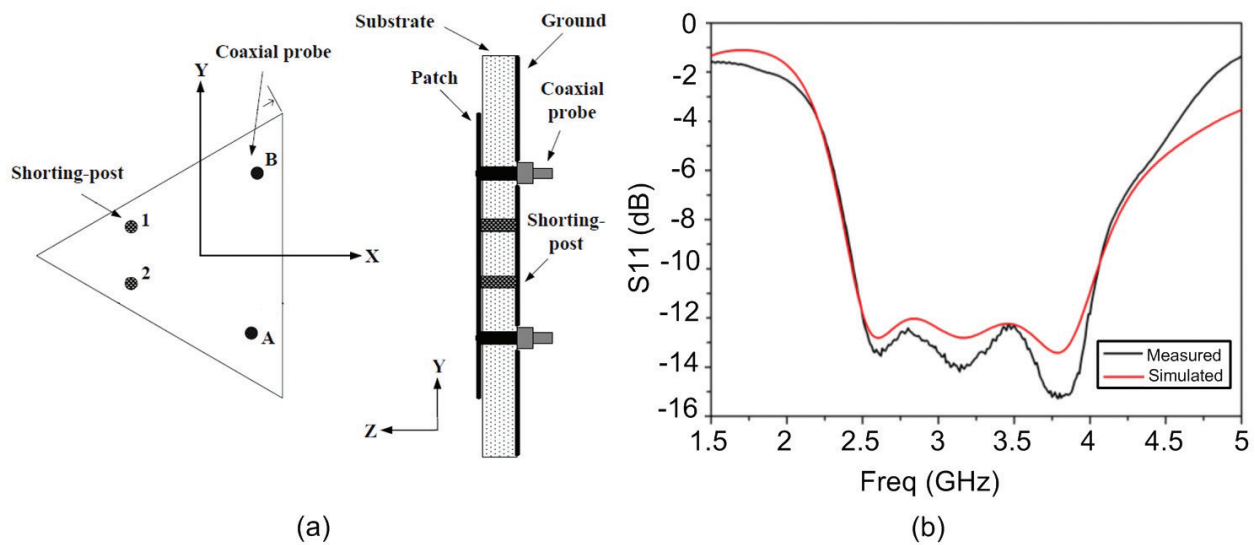


**Figure 41.** The differentially fed equilateral triangular patch antenna loaded by shorting posts which is presented in Ref. [44]. (a). Topology of the structure. (b). Reflection coefficient of a sample antenna designed in Ref. [44].

In Ref. [45], in the same way as presented in Ref. [43], a rectangular patch is differentially fed so that the spurious modes between  $TM_{10}$  and  $TM_{30}$  modes cannot be excited. But here these two modes are coupled to each other by another way. The proposed structure in Ref. [45] is shown in **Figure 42(a)**. In this structure, the shorting pins increase the resonant frequency of  $TM_{10}$  mode without any effect on  $TM_{30}$  mode; however, the pair of long slots shifts down the resonant frequency of  $TM_{30}$  mode with slight effect on  $TM_{10}$  mode. The short centred slot is also used for better impedance matching. By this way, the desired modes  $TM_{10}$  and  $TM_{30}$  could be well-coupled leading to enhancement of the antenna bandwidth. In **Figure 42(b)**, the reflection coefficient of a sample antenna designed in Ref. [45] is shown and about 13% bandwidth can be observed.

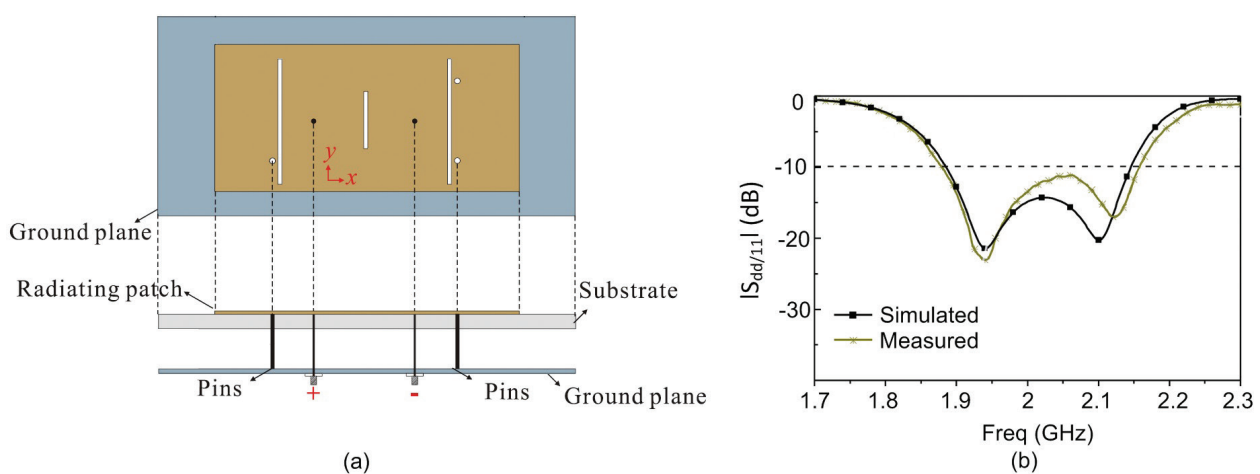


**Figure 42.** The differentially fed rectangular patch antenna presented in Ref. [45]. (a). Topology of the structure. (b). Reflection coefficient of a sample designed in Ref. [45].

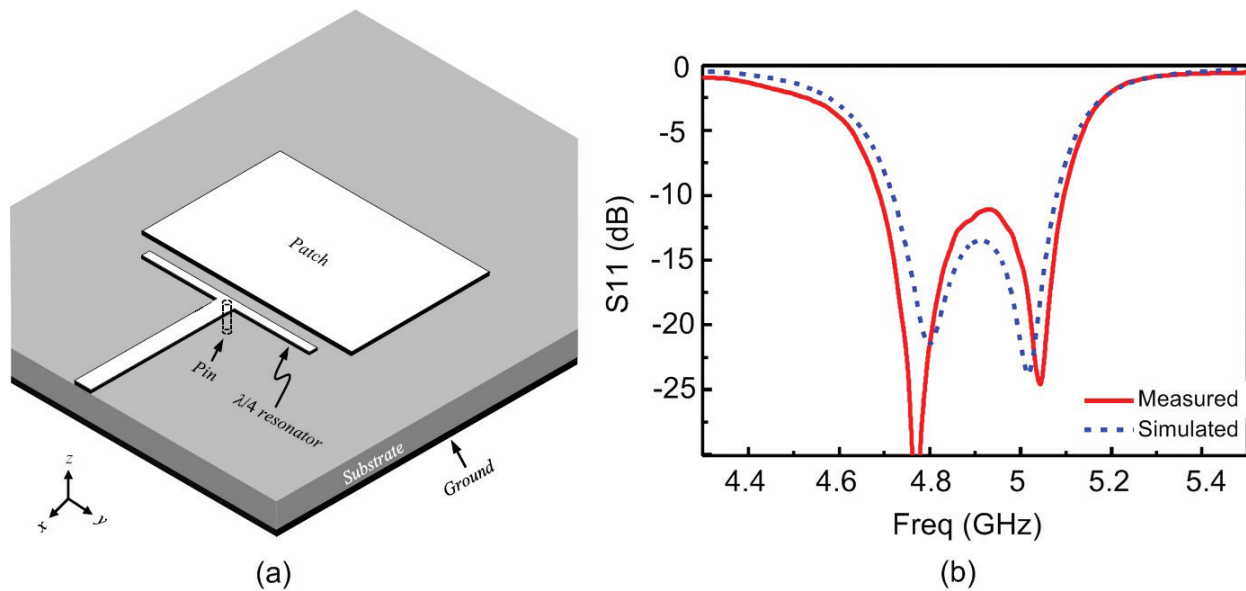


**Figure 43.** The capacitively fed rectangular patch antenna presented in Ref. [46]. (a). Topology of the structure. (b). Reflection coefficient of a sample designed in Ref. [46].

In Ref. [46], as shown in **Figure 43(a)**, the microstrip patch is not fed directly. In this structure, the feed line excites a pair of non-radiating quarter-wavelength microstrip line resonators which are capacitively coupled to the patch. As a result, dual-resonance structure is provided in which the two resonances correspond to the patch and quarter-wavelength microstrip line resonators, respectively. By tuning the gap between the resonators and the patch, a proper coupling between them and consequently wider impedance bandwidth can be obtained. In addition, the shunting pin introduced in the central plane suppresses the excitation of all even-order modes in quarter-wavelength resonators and consequently in the patch. As a result, the  $TM_{20}$  mode which is the most harmful mode that can generate cross-polar radiation is naturally suppressed. In **Figure 43(b)**, the reflection coefficient of a sample antenna designed in Ref. [46] is shown by which the impedance bandwidth of about 8.5% bandwidth could be obtained.

## 9. Summary

In this chapter, a variety of procedures proposed in the literature to increase the impedance bandwidth of microstrip patch antennas are presented and discussed. In Section 2, bandwidth enhancement by proper choosing of substrate is described and declared that up to 10% bandwidth can be obtained using this method taking this fact into consideration that other characteristics of antenna, say efficiency and backward radiation, may be affected. In Section 3, it is shown that by applying indirect feeding mechanism and coupling the electromagnetic fields to the patch, bandwidth can be enhanced. Two methods including proximity coupled and aperture-coupled patches were introduced by which up to 10% and

30% bandwidth can be achieved, respectively. However, for proximity coupled patches, if external matching structure is used, the achievable bandwidth can be doubled. In Section 4, bandwidth enhancement making use of horizontally parasitic elements at the antenna aperture is described and stated that namely 20% bandwidth can be achieved using this single-layer technique at the expense antenna size enlargement which makes it unsuitable for use in array configurations. Sections 5 and 6 explore the stacked patches, a multilayered solution using vertically parasitic elements that can result in very wide bandwidths (namely 50–70%). By this method, the antenna planar size is kept small making it interesting for use in arrays; however, due to its multilayered topology, it has problems with cost and fabrication complexity compared to single-layer solutions. In Sections 2–6, the focus was on linear polarised antennas. Therefore, the solutions for wideband circular polarised patch antennas are introduced and discussed in Section 7. The examples presented in this section reveals that namely up to 20% AR bandwidth can be achieved using the techniques introduced in Section 7. Finally, in Section 8, other techniques proposed in the literature including log-periodic array of patches, E-shaped patch, L-shaped feeding, microstrip monopole slotted antenna, defected ground/patch technique and the latest works in recent years are introduced and investigated. The bandwidth obtained by some designed samples using these structures were 100%, 11%, 50%, 82%, 114% and 50%, respectively.

## Author details

Seyed Ali Razavi Parizi

Address all correspondence to: alirazaviparizi@gmail.com

Department of Electrical and Computer Engineering, Graduate University of Advanced Technology, Kerman, Iran

## References

- [1] Waterhouse RB. *Microstrip Patch Antennas: A Designer's Guide*. Springer Science & Business Media; New York; 2003
- [2] Kumar G, Ray KP. *Broadband Microstrip Antennas*. Artech House; Boston; 2003
- [3] Zurcher JF. The SSFIP: A global concept for high performance broadband planar antennas. *Electronics Letters*. 1988;**24**:1433-1435
- [4] Rathi V, Kumar G, Ray KP. Improved coupling for aperture coupled microstrip antennas. *IEEE Transactions on Antennas and Propagation*. 1996;**44**(8):1196-1198
- [5] Kumar G, Gupta KC. Broadband microstrip antennas using additional resonators gap-coupled to the radiating edges. *IEEE Transactions on Antennas and Propagation*. 1984;**32**:1375-1379

- [6] Kumar G, Gupta KC. Nonradiating edges and four edges gap-coupled with multiple resonator, broad band microstrip antennas. *IEEE Transactions on Antennas and Propagation*. 1985;**33**:173-178
- [7] Chew WC. A broadband annular ring microstrip antenna. *IEEE Transactions on Antennas and Propagation*. 1982;**30**:918-922
- [8] Targonski SD, Waterhouse RB, Pozar DM. Design of wideband aperture stacked patch microstrip antenna. *IEEE Transactions on Antennas and Propagation*. 1998;**46**(9):1245-1251
- [9] Reddy KTV, Kumar G. Dual feed gap coupled square microstrip antennas for broadband circularly polarization. *Microwave and Optical Technology Letters*. 2000;**26**(6):399-402
- [10] Reddy KTV, Kumar G. Gap Coupled Broadband Circularly Polarized Square Microstrip Antennas. In: *International Conference on Computers, Communication and Devices, ICCCD*; 2000. p. 365-368
- [11] Reddy KTV, Kumar G. Stacked square microstrip antennas for wideband circular polarization. In: *National Conf. on Communications, NCC*. Kanpur: Indian Institute of Technology; 2001. p. 125-128
- [12] Huang CY, Wu JY, Wong KL. Cross-slot-coupled microstrip antenna and dielectric resonator antenna for circular polarization. *IEEE Transactions on Antennas and Propagation*. 1999;**47**(4):605-609
- [13] Vlasits T. Performance of a cross aperture coupled single feed circularly polarized patch antenna. *Electronic Letters*. 1996;**32**(7):612-613
- [14] Targonski SD, Pozar DM. Design of wideband circularly polarized aperture coupled microstrip antennas. *IEEE Transactions on Antennas and Propagation*. 1993;**41**(2):214-220
- [15] Pozar DM, Duffy SM. A dual-band circularly polarized aperture-coupled stacked microstrip antenna for global positioning satellite. *IEEE Transactions on Antennas and Propagation*. 1997;**45**(11):1618-1625
- [16] Aksun MI, Chuang SL, Lo YT. On slot-coupled microstrip antennas and their applications for circular polarization operation. *IEEE Transactions on Antennas and Propagation*. 1990;**38**:1224-1230
- [17] Huang CY, Wu CY, Wong KL. Slot-coupled microstrip antenna for broadband circular polarization. *Electronic Letters*. 1998;**34**(9):835-836
- [18] James JR, Hall PS. *Handbook of Microstrip Antennas*. Vol. 1. London: Peter Peregrinus; 1989
- [19] Pozar DM, Schaubert DH. *Microstrip Antennas: The Analysis and Design of Microstrip Antennas and Arrays*. New York: IEEE Press; 1995
- [20] Teshirogi TM, Chujo W. Wideband Circularly Polarized Antenna with Sequential Rotations and Phase Shift of Elements. In: *ISAP*; 1985. p. 117-120

- [21] Lo WK, Chan CH, Luk KM. Circularly polarized microstrip antenna Array using proximity coupled feed. *Electronic Letters*. 1998;**34**(23):2190-2191
- [22] Huang J. A technique for an array to generate circular polarization with linear polarized elements. *IEEE Transactions on Antennas and Propagation*. 1986;**34**(9):1113-1123
- [23] Iwasaki H, Nakajima T, Suzuki Y. Gain improvement of circularly polarized array antenna using linearly polarized elements. *IEEE Transactions on Antennas and Propagation*. 1995;**43**(6):604-608
- [24] Hall PS. Multi-octave bandwidth log-periodic microstrip antenna array. *IEE Proceedings—Microwaves, Antennas and Propagation*. 1986;**133**(2):127-136
- [25] Pues H. Wideband quasi log-periodic microstrip antennas. *IEE Proceedings—Microwaves, Antennas and Propagation*. 1981;**128**:159-163
- [26] Kakkar R, Kumar G. Stagger tuned microstrip log-periodic antenna. *IEEE Antennas and Propagation Society International Symposium. Digest*. 1996:1262-1265
- [27] Yang W, Zhou J. Wideband low-profile substrate integrated waveguide cavity-backed E-shaped patch antenna. *IEEE Antennas and Wireless Propagation Letters*. 2013;**12**:143-146
- [28] Awida MH, Suleiman SH, Fathy AE. Substrate-integrated cavity-backed patch arrays: A low-cost approach for bandwidth enhancement. *IEEE Transactions on Antennas and Propagation*. 2011;**59**(4):1155-1163
- [29] Kuo I-S, Wong K-L. A dual-frequency L-shaped patch antenna. *Microwave and Optical Technology Letters*. 2000;**27**:177-179
- [30] Wang L, Guo YX, Sheng WX. Wideband high-gain 60-GHz LTCC L-probe patch antenna array with a soft surface. *IEEE Transactions on Antennas and Propagation*. 2013;**61**(4):1802-1809
- [31] Latif SI, Shafai L, Sharma SK. Bandwidth enhancement and size reduction of microstrip slot antennas. *IEEE Transactions on Antennas and Propagation*. 2005;**53**(3):994-1003
- [32] Guha D, Biswas S, Biswas M, Siddiqui JY, Antar YMM. Concentric ring shaped defected ground structures for microstrip circuits and antennas. *IEEE Antennas and Wireless Propagation Letters*. 2006;**5**:402-405
- [33] Salehi M, Tavakoli A. A novel low mutual coupling microstrip antenna array design using defected ground structure. *International Journal of Electronics and Communications*. 2006;**60**:718-723
- [34] Guha D, Biswas S, Joseph T, Sebastian MT. Defected ground structure to reduce mutual coupling between cylindrical dielectric resonator antennas. *Electronic Letters*. 2008;**44**(14):836-837
- [35] Arya AK, Kartikeyan MV, Patnaik A. Efficiency enhancement of microstrip patch antenna with defected ground structure. In: *International Conference on Recent Advances in Microwave Theory and Applications, Microwave; 2008*

- [36] Zheng SY, Yeung SH, Chan WS, Man KF, Leung SH. Size-reduced rectangular patch hybrid coupler using patterned ground plane. *IEEE Transactions on Microwave Theory and Techniques*. 2009;**57**(1):180-188
- [37] Kumar C, Guha D. Nature of cross-polarized radiation from probe fed circular microstrip antenna and their suppression using different geometries of DGS. *IEEE Transactions on Antennas and Propagation*. 2012;**60**:92-101
- [38] Kumar C, Guha D. DGS integrated rectangular microstrip patch for improved polarization purity with wide impedance bandwidth. *IET Microwave Antennas Propagation*. 2014;**8**(8):589-596
- [39] Ghosh A, Ghosh D, Chattopadhyay S, Singh LLK. Rectangular microstrip antenna on slot type defected ground for reduced cross polarized radiation. *IEEE Antennas and Wireless Propagation Letters*. 2015;**14**:321-324
- [40] Chiang KH, Tam KW. Microstrip monopole antenna with enhanced bandwidth using defected ground structure. *IEEE Antennas and Wireless Propagation Letters*. 2008;**7**: 532-535
- [41] You W, Guo H, Cai W, Liu X. A D-shaped defected patch antenna with enhanced bandwidth. *IEEE International Symposium on Microwave, Antenna, Propagation and EMC Technologies for Wireless Communications*. 2009:684-686
- [42] Chakraborty S, Ghosh A, Chattopadhyay S, Singh LK. Improved cross polarized radiation and wide impedance bandwidth from rectangular microstrip antenna with dumb-bell shaped defected patch surface. *IEEE Antennas and Wireless Propagation Letters*. 2016;**15**:84-88
- [43] Liu NW, Zhu L, Choi WW, Zhang JD. A novel differential-fed patch antenna on stepped-impedance resonator with enhanced bandwidth under dual-resonance. *IEEE Transactions on Antennas and Propagation*. 2016;**64**(11):4618-4625
- [44] Wang J, Liu Q, Zhu L. Bandwidth enhancement of a differential-fed equilateral triangular patch antenna via loading of shorting posts. *IEEE Transactions on Antennas and Propagation*. 2017;**65**(1):36-43
- [45] Liu NW, Zhu L, Choi WW. A differential-fed microstrip patch antenna with bandwidth enhancement under operation of TM<sub>10</sub> and TM<sub>30</sub> modes. *IEEE Transactions on Antennas and Propagation*. 2017;**65**(4):1607-1614
- [46] Zhang JD, Zhu L, Wu QS, Liu NW, Wu W. A compact microstrip-fed patch antenna with enhanced bandwidth and harmonic suppression. *IEEE Transactions on Antennas and Propagation*. 2016;**64**(12):5030-5037

